

UNIVERSIDADE DE LISBOA
FACULDADE DE CIÊNCIAS
DEPARTAMENTO DE BIOLOGIA ANIMAL



Evaluating and interpreting post-fire Water Quality changes in Portuguese Reservoirs

Niels Nitzsche

Mestrado em Ecologia e Gestão Ambiental

Dissertação orientada por:
Joana Raquel Mendes Cação Parente
João Pedro Carvalho Nunes

2022

Acknowledgments

I am very grateful to my thesis advisors Joana Parente and João Nunes who guided me throughout the whole process of this work. I would like to thank them for their efforts in answering all my doubts and questions over the course of this year, giving me technical and non-technical insights, and even sending me to the EGU General Assembly. I would also like to thank all the people from the FRISCO project who were involved in the work in some form or another. Without their work and advice, this thesis would not have been possible.

Finally, I want to thank my family and friends for their continuous encouragement and support throughout my time as a student and while writing this thesis. Thank you.

Abstract

Wildfires in the Mediterranean, and especially in Portugal have been increasing in extent and frequency over the last years. One of the many impacts of wildfires on humans and ecosystems is on the water quality of surface waters. Ashes and increased erosion rates might elevate the influx of nutrients, sediments, or other water quality-related components, possibly affecting water supply. In this work, time series of eight water quality parameters (biological- and chemical oxygen demand, conductivity, total phosphorous, nitrate, total suspended sediments, dissolved oxygen, and pH) were assessed via changepoint analysis to identify events of post-fire water contamination in over 60 Portuguese reservoirs. Further, possible fire-, watershed-, reservoir-, and climatic drivers were linked with the occurrence of these contamination events through logistic regression using generalized additive models. Results showed changes in all parameters after wildfires with varying frequency. Total phosphorous, nitrate, and total suspended sediments increased in 9.6-13.6 % of all wildfires. Most changes fell into the unusually large wildfire seasons of 2003-2005 and 2017, while the greatest impacts could be seen in southern Portuguese reservoirs after 2005. Fire size was identified as the main driver of post-fire water contamination, while reservoir and climate-related characteristics like water levels also played a major role in some parameters. Increased levels of suspended sediments were identified as a potential threat to water supply, especially when large fires coincide with drought-induced low reservoir water levels. The identification of post-fire water contamination events and their drivers from large datasets may support numerous case and modeling studies and inform water management about possible future threats.

Keywords: wildfires, post-fire erosion, water contamination, changepoint analysis, logistic regression,

Resumo

Os incêndios florestais no Mediterrâneo, e especialmente em Portugal, têm vindo a aumentar em extensão e frequência nos últimos anos. O abandono rural, as florestas não geridas e o aumento do risco de incêndio induzido pelas alterações climáticas conduzirão a um maior número e intensidade de incêndios florestais em Portugal no futuro. A recente onda de incêndios florestais de 2017 foi a maior das últimas décadas, provocando a morte a dezenas de pessoas e a destruição de milhares de metros quadrados, uma realidade que provavelmente se tornará mais frequente nas próximas décadas.

Para além das alterações óbvias na paisagem e ecossistemas, um dos muitos impactos dos incêndios florestais nos seres humanos e no ambiente é a forma como afetam a qualidade das águas superficiais. A deposição de cinzas e o aumento da taxa de erosão do solo podem promover o influxo de nutrientes, sedimentos ou outros componentes para as águas de superfície, deteriorizando a qualidade da água e conduzindo à eutrofização dos albufeiras, o que pode provocar o florescimento de algas e o aumento da mortalidade dos peixes. Por outro lado, podem também afetar, durante longos períodos de tempo, o abastecimento de água devido ao aumento da turbidez das águas superficiais e dos níveis de carbono orgânico, uma vez que o reflorescimento da vegetação é frequentemente lento. Daí que a caracterização de eventos anteriores de contaminação provocados por incêndios florestais pode ajudar na avaliação dos riscos e na determinação das áreas ameaçadas.

Neste trabalho, foram avaliadas as variações temporais de oito parâmetros de qualidade da água (carência biológica e química de oxigénio, condutividade, fósforo total, nitrato, sólidos suspensos totais, oxigénio dissolvido e pH) do Sistema Nacional de Informação de Recursos Hídricos ao longo de um período de mais de 20 anos com o objetivo de detectar eventos de contaminação da água após a

ocorrência de um incêndio florestal. Foram examinados cerca de 120 eventos em mais de 60 albufeiras em todo o país. As variações temporais foram avaliadas através da análise de changepoints, de forma a detectar alterações significativas nos parâmetros que pudessem representar alterações na qualidade da água induzidas pelo fogo. Utilizaram-se três algoritmos diferentes no software R, uma vez que não havia um método único disponível que pudesse lidar com atributos de séries cronológicas (por exemplo, não-normalidade, autocorrelação) sem que possivelmente introduzisse erros na análise.

Após a detecção, a ocorrência dos eventos de contaminação foi modelada através de uma regressão logística usando Modelos Aditivos Generalizados. Dados sobre as características do fogo, bacia hidrográfica, reservatório e clima foram recolhidos e processados para explicar e prever os eventos de contaminação da água após o incêndio. Estes dados incluíram a dimensão e gravidade do fogo, a relação entre a área da bacia hidrográfica e o volume de albufeira, a conectividade dos sedimentos, o índice de aridez, os níveis dos albufeiras, o índice de precipitação normalizado e certas classes de uso do solo.

Em mais de 40% dos eventos selecionados foram identificadas alterações pós-incêndio em pelo menos um dos oito parâmetros de qualidade da água considerados. A frequência das respostas variou consoante o parâmetro analisado, sendo que 5-22% dos eventos resultaram num changepoint após os incêndios florestais. A condutividade foi o parâmetro mais afectado, enquanto que o oxigénio dissolvido foi o que teve menos alterações. A maioria das alterações pós-incêndio foram encontradas após as épocas de incêndios de 2003-2005 e 2017, com as albufeiras no sul de Portugal a serem especialmente afectadas.

A dimensão do incêndio, a conectividade dos sedimentos e os níveis dos reservatórios após os incêndios foram todos identificados como factores significativos, especialmente na modelação dos nutrientes (fósforo e nitrato total) e de sedimentos suspensos totais. Os modelos discriminaram melhor os changepoints de nenhuma reacção nesses parâmetros do que nos outros parâmetros dados os preditores testados com valores da área abaixo da curva de 0.8-0.9. Em geral, a dimensão do incêndio teve o maior efeito sobre a ocorrência ou não de um evento de contaminação pós-incêndio.

Níveis elevados de sólidos suspensos foram identificados como ameaça potencial para o abastecimento de água, especialmente quando incêndios de grandes dimensões coincidem com baixos níveis de água disponível nas albufeiras provocados pela seca. Após a seca de 2004/2005, os níveis de sedimentos suspensos totais nas bacias hidrográficas afectadas por incêndios ultrapassaram largamente os níveis limite, após os quais o abastecimento de água poderia ser afectado. No entanto, os possíveis impactos poderiam ser amenizados pela presença de estações de tratamento de água.

De um modo geral, os eventos de contaminação da água pós-incêndio puderam ser identificados nas séries temporais disponíveis. Os modelos foram também, na sua maioria, capazes de distinguir entre mudança e nenhuma mudança, excepto para os parâmetros de oxigénio dissolvido, condutividade e pH. Estes parâmetros revelaram-se inadequados para identificação de alterações pós-incêndio, mas ainda assim valiosos na avaliação da gravidade das mesmas, quando os eventos de contaminação já estavam identificados. Os outros parâmetros mostraram melhor desempenho e poderá haver potencial para prever o impacto nos sedimentos suspensos através dos preditores utilizados.

A identificação de eventos de contaminação de água pós-incêndio e dos seus promotores a partir de grandes conjuntos de dados pode suportar vários casos de estudo e fornecer as ferramentas necessárias ao setor de gestão da água para prevenir possíveis ameaças futuras. Com as previsões a ditar um aumento significativo de grandes incêndios, bem como da frequência e gravidade dos períodos de secas, o risco de contaminação da água após os incêndios poderá também aumentar nas próximas décadas. Outros trabalhos como este são necessários para confirmar ou questionar os resultados e generalizar os

conhecimentos obtidos com esta tese de modo a facilitar a antecipação da dimensão dos impactos previstos em cenários futuros.

Palavras-chave: incêndios, erosão pós-fogo, contaminação da água, análise de ponto de mudança, regressão logística

Table of Contents

Acknowledgments	II
Abstract	III
Resumo.....	III
Table of Contents	VI
List of Figures	VIII
List of Tables.....	X
List of Abbreviations.....	XI
1 Introduction	1
2 Background	2
2.1 Wildfire effects on water quality	2
2.2 Changepoint analysis in time series	4
2.3 Generalized additive models	5
3 Data and methodology.....	6
3.1 Research goals and study design	6
3.2 Study area	7
3.3 Changepoint analysis.....	10
3.3.1 Reservoir water quality parameter time series	10
3.3.2 Selection of reservoirs and fire events for changepoint analysis.....	11
3.3.3 Changepoint analysis algorithms.....	11
3.4 Logistic regression	13
3.4.1 Logistic regression predictor variables.....	13
3.4.2 Data and variable preparation for logistic regression.....	14
3.4.3 Model Building.....	15
3.4.4 Model evaluation.....	15
4 Results	17
4.1 Burned areas in the study period	17
4.2 Changepoint analysis.....	17
4.2.1 Spatial and temporal distribution of effects.....	19
4.2.2 Quantitative analysis of TSS changepoints	21
4.3 Modelling results.....	22
4.4 Most important model predictor effects	24
4.4.1 Fire size	25
4.4.2 Fire severity.....	25
4.4.3 Sediment connectivity	26
4.4.4 Reservoir levels	27

4.4.5	Further predictors	28
5	Discussion	29
5.1	Parameter responses	29
5.2	Predictor effects.....	32
5.2.1	Main predictors.....	32
5.2.2	Further predictors	33
5.3	Limitations and possible error sources	34
6	Conclusion.....	35
7	Literature Cited.....	37
Appendix	49
A.1	Study area.....	49
A.2	Calculation of watersheds.....	50
A.3	Origin and calculation of regression analysis predictor variables	50
A.4	Missing data before multiple imputation in the predictor and response variables	51
A.5	PCA and Cluster analysis of predictors:.....	53
A.6	Results of the changepoint analysis.....	54

List of Figures

Figure 2.1 Schematic view of the basic effects that wildfires have on water infiltration and sediment erosion. Graphic taken from USGS (2020).	2
Figure 2.2: Basic structure of changepoint analysis methods (adjusted from Truong et al., 2020)	5
Figure 3.1: Graphic of the study design and workflow, with the main achievement, and supplementary goals in green. Inputs are marked in blue, while major work steps are grey.....	7
Figure 3.2: The study area with selected watersheds and different characteristics; a) selected watersheds b) elevation c) Köppen-Geiger climate classification after Beck et al. 2018) d) land use according to the Cartografia de Uso e Ocupação do Solo (COS) 2015 with the general distribution of land use in Portugal e) burned areas from 1980-2018 and the fire recurrence.	8
Figure 4.1: Distribution of the number of affected parameters per wildfire event.	17
Figure 4.2: Cluster analysis of the response variables biological oxygen demand (BOD), chemical oxygen demand (COD), conductivity (Cond.), total phosphorus (TP), nitrate (NO ₃), dissolved oxygen (DO), total suspended sediments (TSS), and pH. Values are given in squared Pearson correlation, which represents the squared phi coefficient for binary variables.	18
Figure 4.3: Affected reservoirs (represented through their watersheds) for the parameters of total phosphorus (TP), nitrate (NO ₃), total suspended sediments (TSS), and conductivity (COND), where red colour indicates a changepoint and grey colour indicates no changepoint in the watershed for any wildfire event. The map on the right displays the maximum number of parameters that were affected for an event. Only the most significant event was chosen to represent a watershed.....	19
Figure 4.4: Detailed map of the number of affected parameters per reservoir (represented through their watersheds) in the most impactful fire event. Visible is a cluster in the south and spread throughout Central and northern Central Portugal.....	20
Figure 4.5: Timeline of analyzed wildfires and events with changepoints in certain WQ parameters. The number of watersheds with no effects (light blue) and with at least one CP (yellow) is also shown, as well as the total BA of Portugal (red line) and the total BA of the analyzed events (black line).....	21
Figure 4.6: Boxplots of the duration of the changepoints (CPs), compared across the two major wildfire seasons (top left), the deviation of the highest measured concentration inside the CP range as a factor of the overall mean over the time series (top right) and the burned area ratio (BAR) of the analyzed events (so independent from CP or no CP) from both wildfire seasons (bottom left).....	22
Figure 4.7: Effects of fire size on the models of biological oxygen demand (BOD), conductivity (COND), total phosphorous (TP), nitrate (NO ₃), total suspended sediments (TSS), and pH. Predicted probabilities for a change are on the y-axis on a scale from 0 to 1, with one being a 100% predicted probability and the fire size on the x-axis in % BAR. The blue line represents the modeled effects. The plots were calculated by setting all other model parameters to their respective mean, to have constant effects. The black lines are confidence intervals that represent the 2.5 and 97.5 percentiles of models from bootstrapped data.	25
Figure 4.8: Effects of different levels of fire severity on the models of chemical oxygen demand (COD), conductivity (COND), total phosphorous (TP), dissolved oxygen (DO), and total suspended sediments (TSS). Probabilities for a change are on the y-axis on a scale from 0 to 1, with one being a 100% predicted probability and the fire severity on the x-axis in % BAR with \geq low; medium, or high fire severity, depending on which predictor resulted in the best fit. The blue line represents the modeled effects. The plots were calculated by setting all other model parameters to their respective mean, to have constant effects. The black lines are confidence intervals that represent the 2.5 and 97.5 percentiles of models from bootstrapped data.	26
Figure 4.9: Effects of the index of connectivity (IC) as a measurement of sediment connectivity on the models of biological oxygen demand (BOD), chemical oxygen demand (COD), conductivity (COND),	

total phosphorous (TP), nitrate (NO₃), total suspended sediments (TSS), and pH. Probabilities for a change are on the y-axis on a scale from 0 to 1, with one being a 100% modeled probability and the IC on the x-axis represented by the 75th percentile value of the IC map in a burnt watershed. The blue line represents the modeled effects. The plots were calculated by setting all other model parameters to their respective mean, to have constant effects. The black lines are confidence intervals that represent the 2.5 and 97.5 percentiles of models from bootstrapped data. 27

Figure 4.10: Effects of post-fire-year reservoir levels on the models of conductivity (COND), nitrate (NO₃), dissolved oxygen (DO), total suspended sediments (TSS), and pH. Predicted probabilities for a change are on the y-axis on a scale from 0 to 1, and the reservoir level on the x-axis as the storage ratio of the maximum storage level. The blue line represents the modeled effects. The plots were calculated by setting all other model parameters to their respective mean, to have constant effects. The black lines are confidence intervals that represent the 2.5 and 97.5 percentiles of models from bootstrapped data. 28

Figure 5.1: Examples of elevated post-fire biochemical oxygen demands that did not get picked up by the changepoint analysis, likely due to high detection limits and only short spikes in the parameters. 30

Figure 5.2: DO concentrations in the Bravura reservoir from 1998-2008. The red lines mark the 2003 fire year, while the orange point marks a local minimum and the red point a global maximum. 30

Figure 5.3: Standardized precipitation index with a 3-month accumulation period values from the European Drought Observatory overlaid onto the conductivity timeline of the Bravura reservoir. Encircled are periods, where large increases in SPI correlate visibly with decreases in COND or vice versa. A lag in the SPI3 time series is caused by the 3-month reference period. 31

Figure 5.4: Predictor effects of IC on the response of total phosphorous (TP) and nitrate (NO₃), excluding an outlier (Penedo Redondo, 2017). Plots were calculated in the same fashion as the effect plots of chapter 4.3. 33

Figure 5.5: Test-wise fire size / watershed-area-to-volume ratio interactions into total phosphorous (TP) and total suspended sediments (TSS) models. Red areas represent a positive impact on effect (so on a changepoint), and dark blue negative impact. Both graphs show positive effects when both fire size and the watershed-area-to-volume ratio were large. 34

Figure AF.1: Detailed map of the analyzed reservoirs and the used sampling stations of the SNIRH network. The names refer to the reservoir names used in SNIRH. 49

Figure AF.2: PCA (left) and Cluster analysis (right) of the predictors. The dashed line in the cluster analysis shows the $r > 0.5$ cut-off. Note that correlation values are shown in r^2 , so the cut-off lies at 0.25 in the graphic. 53

List of Tables

Table 3.1 Selected water quality parameters, what they indicate, and what could be expected post-fire	10
Table 3.2: Characteristics that could influence a response of the water quality parameters. SPI12 is referring to the standardized precipitation index with a 12-month accumulation period, BAR to the burned area ratio, and IC to the index of connectivity.	13
Table 4.1 Number of CPs per parameter and the CP ratio for the biological oxygen demand (BOD), chemical oxygen demand (COD), conductivity (COND), total phosphorus (TP), nitrate (NO ₃), dissolved oxygen (DO), total suspended sediments (TSS), and pH.	17
Table 4.2: Model evaluation scores for the parameter models. The area under the curve (AUC) and root-mean-squared error (RMSE) are based on either 5-fold or 10-fold stratified cross-validation of the calibrated models. Good deviance explained and AUC values are highlighted in bold. Akaike Information Criterion (AIC) and RMSE are seen as comparative quality metrics. Reported are the scores for the fire size-based (FSB) and severity-based (SB) models for the parameters biological oxygen demand (BOD), chemical oxygen demand (COD), conductivity (COND), total phosphorous (TP), nitrate (NO ₃), dissolved oxygen (DO), total suspended sediments (TSS), and pH.	23
Table AT.1: Information on missing data of the predictors. SPI12 represents the standardized precipitation index with a 12-month accumulation period. The index of connectivity (IC) is represented through the 75th percentile, and fire severity through the burned area above a certain Δ normalized burn ratio (NBR).....	51
Table AT.2: Proportion of missingness in the response parameters of biological oxygen demand (BOD), chemical oxygen demand (COD), conductivity (COND), total phosphorus (TP), nitrate (NO ₃), dissolved oxygen (DO), total suspended sediments (TSS), and pH. All parameters show low levels of missingness except for COD.	52
Table AT.3: Results of the changepoint analysis for the parameters biological oxygen demand (BOD), chemical oxygen demand (COD), conductivity (COND), total phosphorus (TP), nitrate (NO ₃), dissolved oxygen (DO), total suspended sediments (TSS), and pH. Orange marks a changepoint with an increase in value/concentration, while blue marks a decrease. The white spots are NAs and grey marks no changepoint in the event.....	54

List of Abbreviations

Δ NBR	Δ Normalized Burn Ratio
AIC	Akaike Information Criterion
AUC	Area under the Receiver Operator Characteristics Curve
BIC	Bayesian Information Criterion
BA	Burned area
BAR	Burned area ratio
BOD	Biological Oxygen Demand
COD	Chemical Oxygen Demand
COND	Conductivity
COS	Cartografia de Uso e Ocupação do Solo
CP	Changepoint
CPA	Changepoint analysis
CV	Cross-validation
DO	Dissolved oxygen
DOC	Dissolved Organic Carbon
FRISCO	managing Fire-induced Risks of Water Quality Contamination
FSB	Fire size based
GAMs	Generalized Additive Models
IC	Index of Connectivity
IC75	75 th percentile of Index of Connectivity maps
mBIC	modified Bayesian Information Criterion
PAHs	Polycyclic Aromatic Carbons
PCA	Principal Component Analysis
RMSE	Root-Mean-Squared Error
SB	Severity based
SDM	Species Distribution Modelling

SNIRH	Sistema Nacional de Informação de Recursos Hídricos
TE	Trapping efficiency
TP	Total phosphorus
TSS	Total suspended sediments

1 Introduction

Wildfires are one of the major natural disturbances to ecosystems worldwide (Lindenmayer et al. 2010, Meurant 2012). Globally, an average of 463 million ha of land burns every year (Lizundia-Loiola et al. 2020). Wildfires have a great influence on the natural carbon- and general nutrient cycles in e.g., forestry ecosystems, and help to remain a balanced system by changing the state of forest succession and influencing biogeography (Neary et al. 2005, Bowman et al. 2009). Fire is also used and greatly affected by humans to e.g., alter land use for agriculture (Tinker et al. 1996), or control fuels in fire-prone areas through prescribed fires (Ryan et al. 2013). These interferences can cause changes in the extent of burned area (BA), fuel, and ignition characteristics of wildfires. Globally, total BA is declining in the recent past due to population increase and the following forest conversion to agricultural lands and landscape fragmentation (Rhoades et al. 2019). However, large, uncontrolled wildfires seem to be occurring more frequently leading to greater media and public attention (Bowman et al. 2009, Wu et al. 2021). Recent examples of catastrophic wildfire events that gained great attention were the Portuguese wildfire season of 2017 with more than 500, 000 ha burned and over 120 casualties (Turco et al. 2019), and the Australian wildfires in 2019-2020 which were unprecedented in its recorded wildfire history (Filkov et al. 2020). Also, in California and the general western United States in 2018 a single wildfire killed more than 80 people, and in 2020 millions of people were affected in some form or the other e.g., through infrastructure loss or air pollution (Blandford 2019, Higuera and Abatzoglou 2021). In the 2021 wildfire season in Greece, an unusually large area was burned (Blandford 2019, Giannaros et al. 2022) and finally, the amazon wildfires of 2019 in Brazil sparked an immediate worldwide outcry. They were however mainly a product of slash and burn practices for farmland conversion (Xu et al. 2021). Human-made deforestation mainly in Brazil then coincided with a drought period, and even more area burned in 2020 (NASA Earth Observatory 2021).

All the earlier named wildfires had in common that they were of unusual size, and magnitude and had unusually destructive effects on their respective regions. This increase in major wildfire events can be partly explained by a climate change-induced increase in fire weather conditions leading to longer and more extreme wildfire seasons (Jolly et al. 2015, Williams et al. 2019, Abram et al. 2021). These climatic drivers will only get stronger in the near future (Jones et al. 2020). Under these conditions, major wildfires are expected to further increase, however, human adaptations to fire regimes and biogeographical adaptations to a changing climate introduce a certain amount of uncertainty into these predictions. Either way, humans need to be prepared for large wildfire events and understand their impacts beyond the most direct causes, to be able to act and react accordingly.

The Mediterranean region is the European wildfire hotspot, and within that the Iberian Peninsula, hosting Spain and Portugal, regularly stands out with the largest BAs (San-Miguel-Ayanz et al. 2021). While wildfires always played a pivotal role in shaping Mediterranean ecosystems, recent increases in large wildfires especially in the Iberian Peninsula are a source of concern (Keeley et al. 2011, San-Miguel-Ayanz et al. 2013). Increases in fire weather risk, an extended wildfire season, rural abandonment and the wide lack of forest management are leading to an increased risk for large wildfires (Beighley and Hyde 2018).

Natural as well as human-caused wildfires have a multitude of direct and indirect effects on people and ecosystems, most notably, the hazards of the fire itself to human life and the economic and ecologic damages caused to buildings, infrastructure, agricultural and forested areas, and resources. While wildfires are mostly detrimental, prescribed fires can also have benefits to ecosystems e.g., through pest and

fuel control or soil fertilization (Pereira et al. 2021). Wildfires also present negative secondary effects, including changes in water quality, posing a risk to ecosystems and water supply. These changes are especially concerning since forests and natural landscapes, where wildfires usually occur, are responsible for a major amount of the world’s clean drinking water supplying more than four billion people (Millennium Ecosystem Assessment 2005, Bladon et al. 2014, Hallema et al. 2019). Extensive knowledge of post-fire water contamination processes and likelihoods is needed to reduce the risks for water supply and water use out of forested ecosystems for the public. Especially, since rising global water stress and a higher number of severe wildfires could enhance future risks of post-fire contamination episodes (Bladon et al. 2014, Martin 2016, Nunes et al. 2018, Robinne et al. 2018, Hallema et al. 2019, Rhoades et al. 2019).

2 Background

2.1 Wildfire effects on water quality

Wildfires can affect both water quality, and the quantity of surface water resources. In rivers and lakes, a multitude of different effects can lead to hydrological responses and deprived water quality (Shakesby and Doerr 2006, Smith et al. 2011). Through regional differences in e.g., fire behavior, climate, and dominant post-fire erosion processes, fire effects have to be interpreted in the local context (Shakesby 2011, Nunes et al. 2018). However, the following description of effects is kept broad enough, so that described effects may also apply to regions in similar climates. A focus however is given on effects that have been reported in the Mediterranean context.

River flows after wildfires are often enhanced through the absence of vegetation cover which normally uptakes and transpires or intercepts rainwater (Figure 2.1). Coupled with at times altered soil characteristics through the burning, surface outflows from wildfire-affected areas can be increased (Soto et al. 1991, Prosser and Williams 1998). Decreased interception and increased surface flow further lead to smaller response times in throughflow after precipitation events, so faster, higher throughflow spikes can be expected (Cerdà 1998, Shakesby and Doerr 2006).

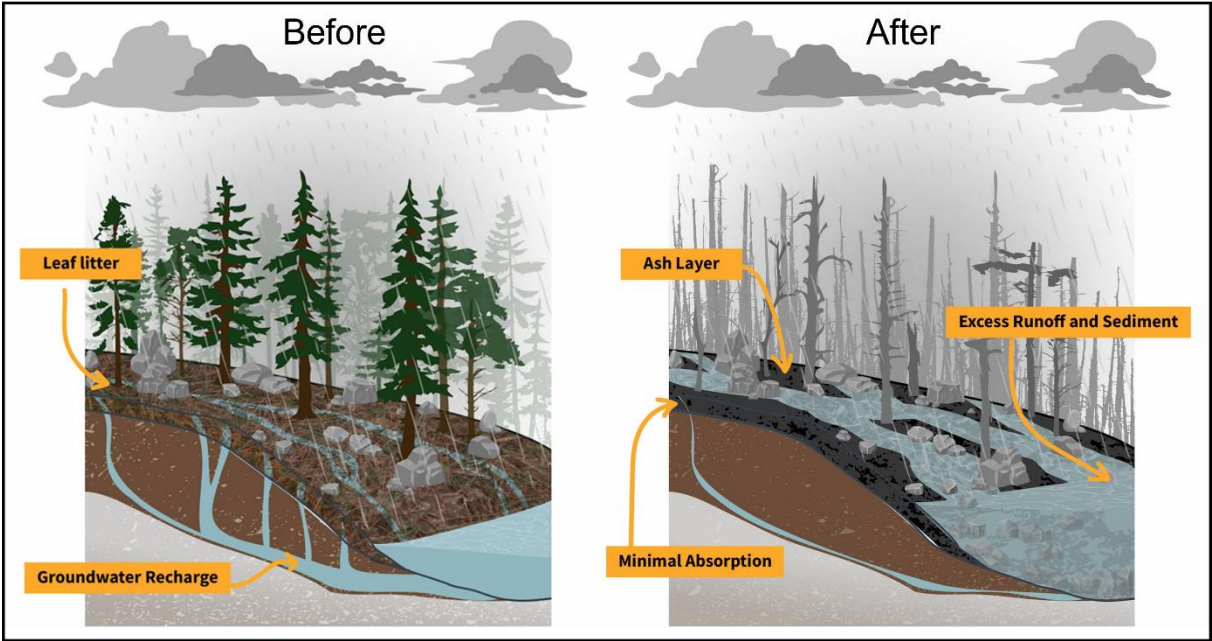


Figure 2.1 Schematic view of the basic effects that wildfires have on water infiltration and sediment erosion. Graphic taken from USGS (2020).

The increased surface flow and reduced vegetation cover enhance soil erosivity, which brings an increased number of particles and nutrients to streams (Blake et al. 2009). This holds true even though nutrients like phosphorous and especially nitrogen are lost to the atmosphere during combustion (Johnson et al. 2007). Together with the ashes produced by the fire, enhanced erosion is the main driver of post-fire water contamination (Smith et al. 2011). While the reduction of vegetation cover increases rainfall erosivity and subsequently soil erosion, burning also changes the characteristics of the soil beneath (Beatty and Smith 2013). Numerous articles report an increase in soil-water repellency after burning (e.g., Neary et al. 2005, Varela et al. 2005, Shakesby and Doerr 2006). This leads to a further decrease in infiltration and therefore increases surface flow and the erosivity of that surface flow. Mechanisms are however largely studied under laboratory or controlled conditions and soil responses may vary depending on the burn temperature (Neary et al. 2005, Shakesby and Doerr 2006, DeBano and Krammes 1966). Further, wildfires can alter soil agglomerates making the soils either more or less susceptible to erosion, but agglomerate stability is generally also correlated to hydrophobicity and so ultimately burn conditions (Guerrero et al. 2001, Mataix-Solera and Doerr 2004).

The quantitative influence of ash on the post-fire water quality response is largely unstudied and interactions of water soil and ashes are complex. Ashes may reduce surface runoff in the first few fire events through the hydrophilic properties of the ash layer, while in the long run, they can clog soil pores to reduce infiltration (Woods and Balfour 2010). After burning the ashes settle on the soil creating a highly erosive layer that gets washed into surface waterbodies or infiltrates topsoil layers (Shakesby 2011). In the Mediterranean context, these ashes often erode quickly (Shakesby 2011). The impact of enhanced post-fire soil erosion often lasts multiple years until vegetation has regrown and erosion rates are back to pre-fire levels (Prosser and Williams 1998). In the Mediterranean, vegetation regrowth times are relatively long so disturbances from burned sites as long as 7 to 10 years have been reported (Mayor et al. 2007, Shakesby 2011). To what extent a post-fire water contamination event is triggered by ashes rather than erosion often is unclear, as effects can overlap in the first years(s) and thorough modeling studies that include both ash availability and transport after fires are only slowly starting to emerge (e.g., Neris et al. 2021).

The introduction of sediments and ashes into streams and waterbodies can have severe negative effects on the ecosystems and water supply (Robinne et al. 2021). Introduction of nutrients, dissolved organic carbon (DOC), pathogens like viruses and bacteria, and otherwise harmful chemicals like trace elements or polycyclic aromatic hydrocarbons (PAHs) are a problem, as well as quickly changing oxygen levels and temperatures of surface waters (Fowler 2003, Bladon et al. 2014, Mansilha et al. 2014). Contaminants either quickly dissolve in the water or bind to fine sediment particles that don't or only slowly sink to the bottom and leach into the water over time (Son et al. 2015). These suspended sediments further increase turbidity, which gives the water a cloudy look. Water supply is at risk as the more turbid and DOC-laden water is not only unpleasant on the eye, but higher chemical loads are needed for disinfection (Martin 2016). The pathogens that are bound to sediment particles are harder to eliminate, which increases the costs of pre-treatment to the point where water supply can be at risk of failure (Robinne et al. 2021). High nutrient levels can also pose a threat to water supply but concerning concentrations for human health are more often expected in groundwater resources from agricultural lands than in surface waters (Bijay-Singh and Craswell 2021). Both nitrate and phosphorous are mainly a threat to aquatic ecosystems. Heightened nitrate, carbon, and especially phosphorous levels can lead to water eutrophication and algae blooms (Schindler 2012). These can be dangerous for fish species and other aquatic biota, as the algae blooms lead to oxygen depletion. Mass mortalities of fish can be the consequence (Schindler 2012, Bladon et al. 2014). A further trigger for oxygen depletion is a heightened oxygen demand caused by the high input of carbon-rich partially and reduced particles from ashes and

burned soil. These bonds get oxidized by microorganisms or through chemical processes which consume dissolved oxygen of water bodies (Dahm et al. 2015). Other contaminants like trace elements, or PAHs can be toxic for aquatic species and humans as not all water treatment plants can eliminate them thoroughly. They could also get enriched in directly exposed species and make their way into the food chain (Abraham et al. 2017b).

Research on post-fire water quality really only came up in the 1970s in North America (Lotspeich et al. 1970). The topic gained more attention in the 1980s, but research was still focused on case study reports or reviews almost exclusively from North America (e.g., Tiedemann et al. 1978, Tiedemann 1979, Schindler et al. 1980). Further case studies took place in the 1990s and 2000s as international interest in the topic slowly grew with notable efforts outside of North America (e.g., Britton 1991). In Europe, more emphasis was and still is put on studying post-fire soil erosion and possible sediment outputs into surface waters than on the impacts in these surface waters. Because of that, a lot of European-based research in post-fire water quality is based on the understanding of changes in soil-water interactions and soil erosion processes after wildfires (Doerr and Cerdà 2005, Shakesby and Doerr 2006). This knowledge is gained through laboratory work and either designed field or case studies. Today work on the topic still mostly consists of these pillars, namely the report of case studies after certain wildfires and laboratory or controlled field studies to understand soil and erosion processes, which are documented in extensive literature reviews (e.g., Shakesby and Doerr 2006, Smith et al. 2011). These are now supported by watershed or sub-basin modeling studies, where nutrient and sediment exports after wildfires are modeled and linked to possible water quality changes (e.g., Basso et al. 2021). However, there are still very few data-based studies that could help to identify the overall susceptibilities of watersheds to post-fire water contamination or quantify such episodes across space and time. Notable recent exceptions are e.g., the studies from Rust et al. (2018) where the authors found that almost one in three analyzed wildfire events in the Western United States resulted in changes in water quality. Or Hallema et al. (2018) who stated, that wildfires with a burned-area ratio (BAR), i.e. the percentage of watershed area that burns during a wildfire or year, of at least 19% are needed to imply structural changes in water availability downstream. Often basin- or sub-basin-focused case studies reveal large differences in post-fire water quality response, so analyses of large data sets are needed to filter out probabilities, generalities, or in this case drivers of post-fire water quality changes. The recent wildfires in California and Australia showed that there is a strong urge to include post-fire water contamination into wildfire research and develop frameworks, as partial shortages and water outages resulted from ash loaden water clogging up freshwater supply (Robinne et al. 2021).

2.2 Changepoint analysis in time series

Changepoint detection has a broad and interdisciplinary field of use as a way to detect transitions of underlying distributions in data series (Chen and Gupta 2012). They are a great tool to discover shifts in time series such as signs of climate change in meteorological time series or medical conditions in electrocardiogram series, independent of temporal resolution (Aminikhanghahi and Cook 2017). Often routinely taken, hydrological time series are suited for studying changes in hydrological systems and were used as early as 1975 (McGilchrist and Woodyer 1975). The approach to detect post-fire water quality changes in routinely sampled water quality time series however is just emerging and was first implemented by Rust et al. (2018).

Changepoint analysis (CPA) methodologies can generally be split into three steps (Truong et al. 2020): a test statistic (or cost function), a search method, and a penalty (Figure 2.2). The test statistic is used to estimate the goodness of fit of a changepoint model i.e., a defined number of structural changes at defined locations (Bai and Perron 2003, Eckley et al. 2011). The cost function may calculate a score for

each of the possible changepoint combinations however it is not advised to go through all possible combinations. In a time series $x_1, \dots, x_t \in \mathbb{R}$ there could be $t-1$ changepoints at $t-1$ different locations. If one would like to find the best possible solution only by using the cost function, 2^{t-1} combinations would have to be considered, which leads to high computational expenses (Killick et al. 2012). A solution to this problem is to use search techniques. These can be accurate through e.g., testing all possible solutions or pruning, or they could be approximate, through iteratively testing only parts of possible combinations (Truong et al. 2020). A penalty term then is included to compare models with different amounts and locations of changepoints and choose the appropriate number of changepoints most often through different information criteria (Akaike Information Criterion (AIC), Bayesian Information Criterion (BIC), modified Bayesian Information Criterion (mBIC), etc.) (Emiliano et al. 2014, Truong et al. 2020). Information criteria are considering the goodness of fit and the number of parameters used, with fewer parameters leading to a preferred model. Different information criteria penalize the use of parameters differently leading to varying results (Emiliano et al. 2014). In the case of changepoint models, the number of parameters refers to the number of changepoints. When the goodness of fit and number of changepoints are optimized, a minimum information criteria score is reached.

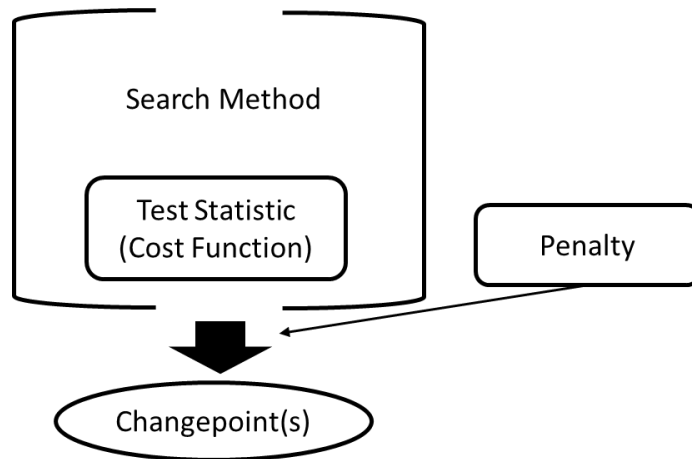


Figure 2.2: Basic structure of changepoint analysis methods (adjusted from Truong et al., 2020)

2.3 Generalized additive models

Linear models belong into the field of statistical learning and are used to describe (regress) an unknown variable Y through its linear relation with other known variables X_j through (Nelder and Wedderburn 1972, Stanton 2001). In their basic form they can be expressed through (Nelder and Wedderburn 1972):

$$y_i = \beta_0 + \sum_j \beta_j x_{ji} \quad (2.1)$$

Where β marks the parameters to calculate the relationship between X_j and Y . Generalized additive models (GAMs) are an extension of these regression models in order to include non-linear effects (Wood 2006). They are more flexible in their use than (generalized) linear models, as they don't rely on linear relationships between predictor and response variables, but can fit nonlinear "smooth" functions s for β so that the relationship becomes (Wood 2006, Wood 2011):

$$y_i = \beta_0 + \sum_j s_j(x_{ji}) \quad (2.2)$$

Together with generalized linear models, they are increasingly used to explain and predict events e.g., in the fields of biology, medicine, or the financial sector (Taylan et al. 2007). Logistic regression is used when the distribution of the response variable Y is binomial. The goal of logistic regression is to establish

a regressive relation between the predictor variable(s) (in this work: fire, climate, and watershed characteristics) and the probability of something occurring or not occurring (in this work: a change in water quality). The explanation of qualitative effects between environmental predictors and a response is arguably most used in species distribution modeling (SDM) (Miller 2010). Here, the presence or absence of an animal species in a certain space and time is explained through relationships with environmental data (see e.g. Manel et al. 1999, Pearce and Ferrier 2000). However, other fields including hydrology, social sciences, medical research, etc. have been successfully using this approach as stochastic modeling approaches are getting more and more popular (e.g. Stagge et al. 2015 linked the occurrence of drought impacts with drought indices).

3 Data and methodology

3.1 Research goals and study design

This work is part of the FRISCO project (short for managing fire-induced risks of water contamination), which studies post-fire contamination pathways, watershed responses, and the possible effects of management strategies. In my work, I focused on the detection of impacts in eight of the most often reported water quality parameters also based on, or limited through, the availability in the used dataset. These include nutrients and other physio-chemical parameters. The study design aims at detecting contamination events in raw time series data of these parameters in different reservoir stations (Figure 3.1). The focus on reservoirs stems from the quality of available data. The sampling frequency of the time series is low (monthly) so events might go unnoticed, as rivers react quickly to runoff events (hours or days). Longer water residency times in reservoirs might lead to higher detection probabilities, even though amplitudes are smaller due to dilution effects. After the detection of contamination events, drivers of these events will be explored, through regression modeling. The main research goals were:

- The identification of past post-fire water contamination events based on fully available time series data in Portuguese reservoirs.
- The identification of wildfire, watershed, climatic or reservoir characteristics as drivers behind these contamination events and their effects.

More so, results can be characterized into temporal or spatial clusters to identify possible risk hotspots or special risk scenarios for post-fire contamination episodes. A further aim of this research is to discuss implications for water supply, however without answering this question, as this is beyond the scope of this work and would need thorough information on water supply and treatment stations of affected reservoirs.

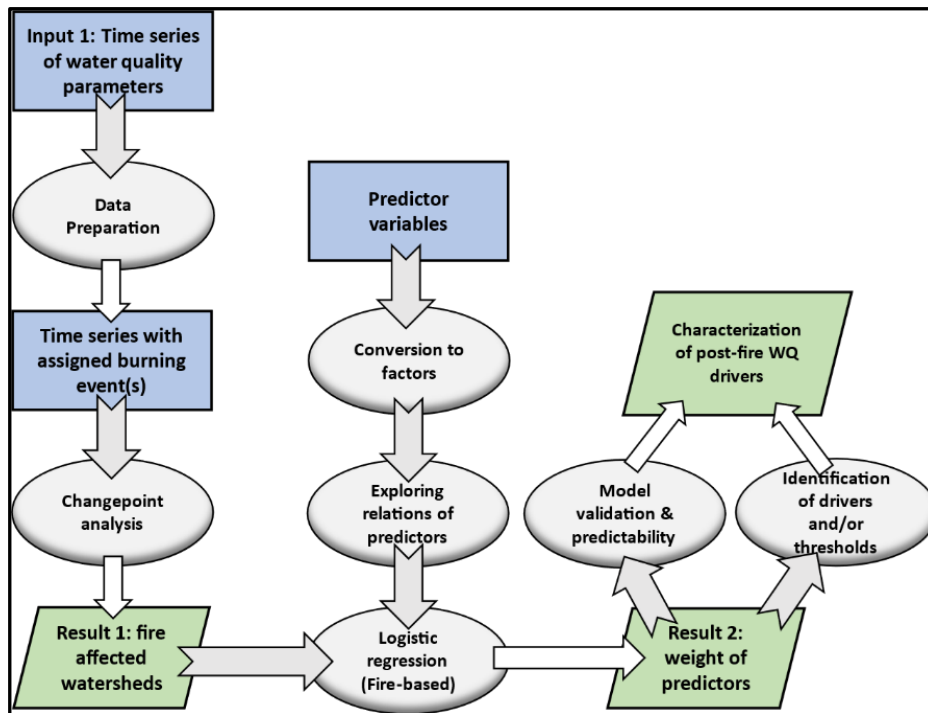


Figure 3.1: Graphic of the study design and workflow, with the main achievement, and supplementary goals in green. Inputs are marked in blue, while major work steps are grey.

3.2 Study area

For this data-driven work, watersheds all over continental Portugal were considered (Figure 3.2a; a more detailed figure with reservoir names and used sampling stations can be found in Appendix A.1 Study area, Figure AF.1). The country is located at the western end of the European continent between Spain and the Atlantic Ocean. The coastal regions and the general Northwest are densely populated while the eastern regions remain sparsely populated (see urban areas in red in Figure 3.2d). The climate in Portugal can be described into two different zones. It is classified into the Köppen-Geiger types Csb, and Csa, subtypes of a temperate dry climate (Beck et al. 2018). The main differences between the Csa and Csb subtypes are the differences in summer temperature with summers being colder (<22°C in the warmest month (Csb)) in the coastal zones and the north of the country. The Portuguese Institute of the Sea and the Atmosphere even identified a third climate type (BSk; cold semi-arid steppe) for the period of 1970-2000 in the south-east Alentejo, pointing towards an even warmer and drier climate in that region (IPMA).

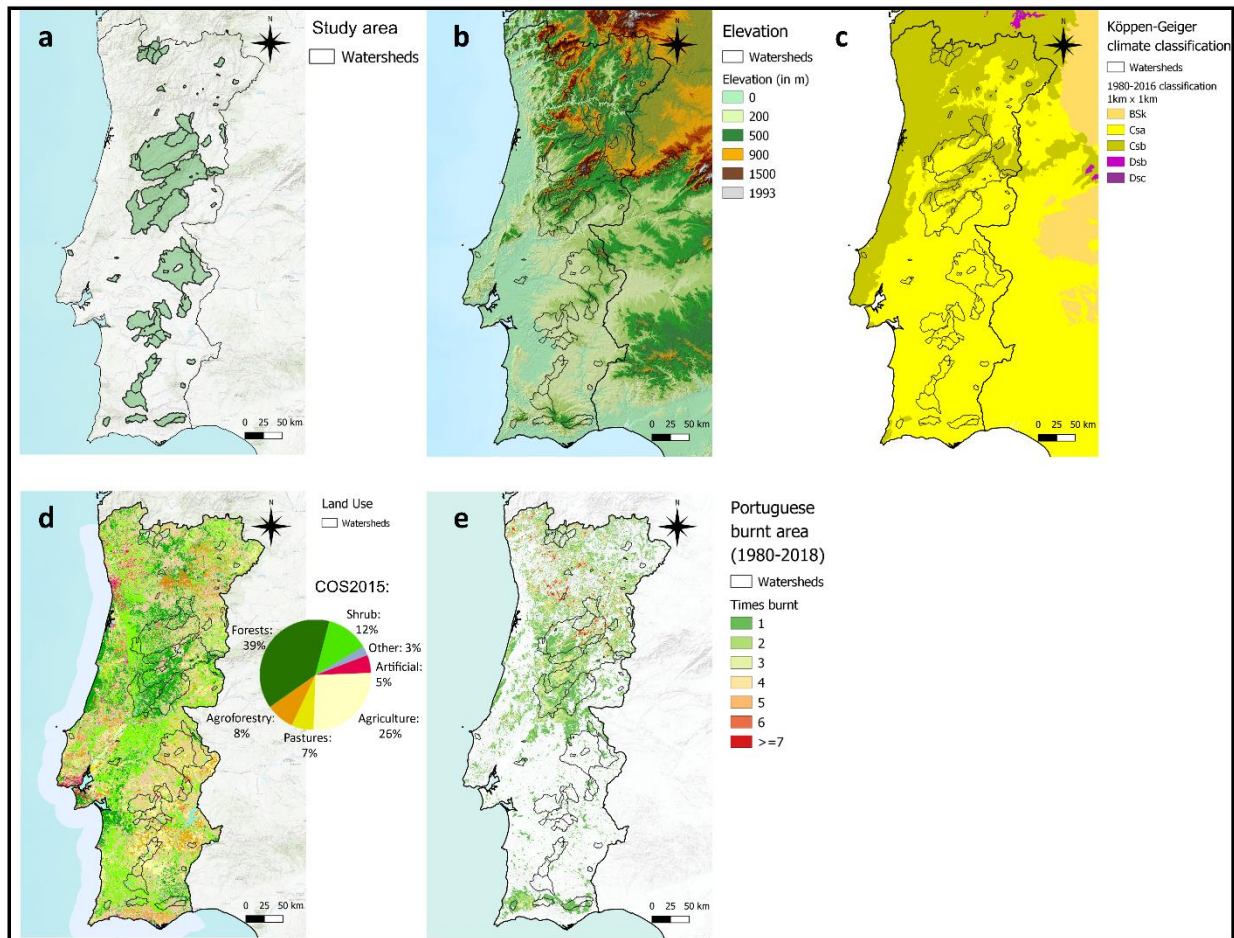


Figure 3.2: The study area with selected watersheds and different characteristics; a) selected watersheds b) elevation c) Köppen-Geiger climate classification after Beck et al. (2018) d) land use according to the Cartografia de Uso e Ocupação do Solo (COS) 2015 with the general distribution of land use in Portugal e) burned areas from 1980-2018 and the fire recurrence.

Nearly 1% of the Portuguese area is burned by wildfires every year (from 1980 to 2020), making it the most affected country in Europe in terms of BAR (San-Miguel-Ayanz et al. 2021). While worldwide BA as well as the BA of other Mediterranean countries seems to be declining over the past decades and century due to fire suppression and land use changes, signals for Portugal are mixed (Yang et al. 2014, Turco et al. 2016, Silva et al. 2019). Especially the 2017 wildfire season has been unusual with the largest BA in recent decades (San-Miguel-Ayanz et al. 2021). Population shifts to urban areas are leading to unmanaged forests and therefore higher fuel loads (Beighley and Hyde 2018). Coupled with generally high human-caused ignition rates Portugal has, “one of the highest forest fire risk rankings in Europe” (Catry et al. 2009, Beighley and Hyde 2018). Future landscapes and ecosystem services of these abandoned lands will be partly shaped by the recurrent fires (Santana et al. 2010, Moghli et al. 2021) and coming wildfire seasons will show if 2017 was an exceptional year or if years like this will become more common.

Regarding the fire regime, Portugal can be divided into two different pyro regions which can lead to differences in BA of a wildfire and the general ignitions as well as different seasonal patterns (Trigo et al. 2016). The northwest of the country is relatively cold and wet with high plant activity and therefore has a slightly different fire regime than the rest of the country. Peak wildfire season in this region is in August when almost 1% of the total area is burned each year, while a second much smaller peak can be found in March (Trigo et al. 2016). For the rest of Portugal, a peak in March is far less prominent while

the highest wildfire activity also falls into the month of August, although with a much lower relative BA (~0.3% of total area). The historic BA in Figure 3.2e also suggests a greater proportion of BA and a much higher frequency of ignitions in the north of the country. Still, some areas in the south contribute significantly to the BA with often large fires (Nunes et al. 2016). The BA patterns coincide well with mountainous areas (see Figure 3.2b and e). The biggest parts of the BAs of southern Portugal are situated in the Serra the Monchique mountains in the western Algarve and the Serra do Caldeirão mountains north of Faro. In the future climatic shifts and changes in fire weather tend to move the pyro regions towards the northern and coastal regions (Calheiros et al. 2021). This could for example mean less frequent but large summer wildfires for the northern regions.

Concerning usual fire patterns in Portugal shrublands are the most burned and therefore also the most at-risk land use class followed by mixed, broadleaf, and coniferous forests (Nunes et al. 2005, Marques et al. 2011). Agricultural areas and pastures on the other hand have only minimal risks of burning. Also, the differences in burn-likeness of certain land use types over others diminish when wildfires are big (Nunes et al. 2005). The often-criticized eucalypts plantations seem to have no explicitly measurable effect on wildfire patterns (Fernandes et al. 2019). Shrubland and forests dominate the watersheds in the north while further south near Coimbra and the Serra de Estrela mountains the landscape is dominated by forests. In the central and southern parts shrubland is more abundant but never exclusively present (Figure 3.2d).

Areas at risk of post-fire water contamination would be most likely situated in areas with high wildfire activity, so in this instance in the North and Central parts of Portugal. The very south could be also at risk since less frequent but usually large wildfires are present and soils could erode even with less severe wildfires due to the lower vegetation cover. These areas are already identified as areas with a high risk of post-fire soil erosion (Parente et al. 2022a), and since this might be the main source of post-fire water contamination similar patterns could be expected.

Water supply in Portugal is handled through different private and publicly owned water companies. Historically, water supply in Portugal consisted of a multitude of uncoordinated well structures to supply local communities, fields, or just your own grounds. In a shift to increase general water quality as well as the consistency of said quality, suppliers turned to reservoirs as a primary water resource as water can be distributed from one source to a large number of consumers while water quality can be controlled and maintained with relatively low effort (Nunes et al. 2006). This helps to ensure a stable and high-quality water supply. Although exact numbers are hard to find, in Portugal surface water is increasingly being used for water supply. While pre-2000 around 40% of water supply was based on surface waters, this number increased to around 70% in 2005-2007 (Jesus 2001, Hulsmann 2011). Before distribution, communal water from reservoirs is often treated extensively in multilevel treatment plants, where it is filtered and disinfected. The country's most important drinking water reservoir is the Castelo de Bode reservoir, which sits between the districts of Castelo Branco and Santarém. It supplies the municipality of Lisbon with drinking water and is located in a fire-prone area, with three major wildfire seasons in the past 20 years (2003: 32% BAR; 2005: 14% BAR and 2017: 33% BAR) making it possibly susceptible to post-fire water contamination. Information on the frequency and size of post-fire contamination events is needed and could help water managers with decisions on the scale of pre-treatment plants.

Reservoirs are also extensively used for agricultural irrigation, but water quality standards for irrigation waters are well below those for water supply (Ayers and Westcott 1985). Crops could be at risk from higher salinity, nutrient load, or toxic trace elements, but these issues are normally not the focus of studies on post-fire water contamination.

3.3 Changepoint analysis

3.3.1 Reservoir water quality parameter time series

The time series used in this work were obtained from the Sistema Nacional de Informação de Recursos Hídricos (SNIRH available at snirh.apambiente.pt). The SNIRH is directly maintained and operated by the Portuguese Environmental Agency and its main objective is the assessment and monitoring of Portuguese water bodies and hydrologic resources. This is achieved through a network of measuring stations all over the country. Of interest for this work was data on water quality and hydrometry (mostly reservoir level data) from reservoir stations. Water quality-related parameters were selected for analysis because of their already established direct or indirect links to post-fire water quality changes and their data availability across a large number of stations in SNIRH (Earl and Blinn 2003, Neary et al. 2005, Smith et al. 2011, Dahm et al. 2015). These included chemical and physical parameters (Table 3.1), namely biological oxygen demand (BOD), chemical oxygen demand (COD), total phosphorus (TP), nitrate (NO₃), dissolved oxygen (DO), total suspended sediments (TSS), pH and conductivity (COND). The time series were made up of monthly sampling at inconsistent intervals, so samples were not taken at the same time and day each month. Data gaps of one to a few months were common and data quality varied between the different reservoirs and parameters. Further, values below varying detection limits were common in the time series, mostly for the parameters of BOD, COD, TP, NO₃, and TSS and sporadically for COND or DO. Different detection limits in a single time series were common. Regarding these limits, COND, DO, and pH all had on average <5% of their observations of a time series below a detection limit while for COD, P, NO₃, and TSS this value was at 30-46%. CBO had by far the highest number of observations below a detection limit, with an average of 59% per time series.

Table 3.1 Selected water quality parameters, what they indicate, and what could be expected post-fire

Parameter	Indicates	Expected effects
Biological Oxygen Demand (BOD)	Partially burned organic matter	Increase mostly through microbial aerobic decomposition of partially oxidized organic matter (Dahm et al. 2015).
Chemical Oxygen Demand (COD)	Reduced matter/metals	Increase mostly through chemical oxidization of previously burnt (reduced) metals or matter (Dahm et al. 2015).
Conductivity	Ionic activity, soluble parts from ashes and sediments	Increase through an increase in ions from soil and organic matter (Earl and Blinn 2003, Emmerton et al. 2020).
Total Phosphorus (TP)	Nutrient enrichment	Increase through higher sediment and organic matter export and leaching (Neary et al. 2005, Lane et al. 2008, Smith et al. 2011).
Nitrate (NO₃)	Nutrient enrichment	Increase through higher sediment and organic matter export and leaching, less consumption through vegetation cover (Neary et al. 2005, Lane et al. 2008, Smith et al. 2011).

Dissolved Oxygen (DO)	Organic and reduced matter	Decrease through an increase in BOD and COD (Dahm et al. 2015).
Total Suspended Sediments (TSS)	Sediment erosion, ashes	Increase through erosion and the introduction of ash (Smith et al. 2011, Burke et al. 2013).
pH	Ashes; burning of organic matter	Mostly increased in soil, could increase or decrease in surface waters (Granged et al. 2011, Abraham et al. 2017a).

3.3.2 Selection of reservoirs and fire events for changepoint analysis

Fire events (in this work defined as all fires in a watershed over a year) were selected in a span of 33 years (1985-2018) out of around 500 stations in over 150 reservoirs, even though wildfires before 1998 are strongly underrepresented as the time series data often lacked sufficient quality in this period. Only one station per reservoir and fire, if possible close to the reservoir outlet was considered, to not inflate the CPA. Only reservoirs with at least six years of continuous data and at least four observations per year were considered, to have no less than three years of pre- and post-fire data. The watersheds of these reservoirs were calculated and overlaid with the yearly BA. Information about the exact calculation of the watersheds can be found in Appendix A.2 Calculation of watersheds. Wildfire events to analyze were picked based on the yearly BAR, to include the most major fires in the period. The only restrictions to choosing an event were that in a 5-year pre- and post-fire period no other wildfire >10 % BA of the watershed could occur. This value was taken as it represents half of what Hallema et al. (2018) identified as a threshold (19% BAR) after which hydrology in the US changed. When only multiple small fires (<10% BAR) occurred over the years, the largest yearly BA was chosen as an event to analyze.

Some exceptions were made with back-to-back years where the effects of two wildfire years were added up and handled as a single fire in the CPA and logistic regression. This can be justified through generally long vegetation recovery rates and therefore long exposure to higher sediment erosion in BAs (Shakesby 2011, Petropoulos et al. 2014), which e.g., was likely enhanced for the 2003-2005 wildfire seasons due to drought conditions (Gouveia et al. 2012). There were only four cases (Caniçada 2009-2010, Castelo de Bode 2003-2005, Funcho 2003-2004, and Salamonde 2010-2011) where this happened, but they included major wildfires and were therefore important for the analysis.

3.3.3 Changepoint analysis algorithms

The water quality parameter time series were analyzed with CPA. For this work, only changes in the mean of the underlying distribution were of importance, as a sharp spike or drop in the concentration or level of a parameter will affect the mean of the distribution. Three different algorithms were used for the computation of a changepoint (CP), the point at which the underlying distributions of the data change. CPA, like most statistical analyses, relies on general assumptions about the underlying data structure (assumptions for parametric CPA given in Chen and Gupta 2012). The assumptions important in the context of this work were:

- Independency of the data (no autocorrelation)

- Normality of the data in each segment

Water quality parameter time series are often, but not always autocorrelated with seasonal autocorrelation being possible (Darken et al. 2002). Additionally, the time series used in this work are partly incomplete, so measurements were not always taken monthly and not always on the same day of a month

leading to difficulties in assessing the autocorrelation. Also, the data is often nonparametric, while a majority of CPA algorithms rely on normality (Truong et al. 2020). As of yet to my knowledge, there is no ready-to-use methodology that incorporates all of these problems so I resorted to using different algorithms that can each handle certain aspects of the problem.

Before analyzing, the samples that were under the detection limit were set to the value of the highest detection limit in the time series and then halved. Dividing the detection limit by two is recommended by the United States Environmental Protection Agency (1996), while different detection limits would introduce a chance for a false positive changepoint due to the jump in mean from one limit to another. Further, to clarify if the time series data was parametric, the residuals of a test-wise CPA were assessed for normality through a Shapiro-Wilk-test (Shapiro and Wilk 1965) and the autocorrelation, as well as the partial autocorrelation, were checked. A CP was attributed to the wildfire if it happened in the fire year itself or in the post-fire year (in the drought scenario of 2004/2005 up to two years after the fire, since a lack of precipitation might produce a lag in the reservoir response). Finally, a changepoint was accepted when two out of three methodologies detected a changepoint in the given period. Using only one method could potentially introduce bias by overestimating changepoints in a certain data type (e.g., when autocorrelation is present).

The computation of the changepoints was done in R (R Core Team 2021) using the packages ‘changepoint’ (Killick and Eckley 2014), ‘changepoint.np’ (Haynes et al. 2016), ‘EnvCpt’ (Killick et al. 2021), ‘strucchange’ (Zeileis et al. 2002) and ‘bcpa’ (Gurarie 2014), while the first three are using similar approaches. The ‘changepoint.np’ package was used because of its ability to deal with nonparametric data which is implemented through a maximum likelihood-based cost function proposed by Zou et al. (2014) and implemented by Haynes et al. 2017b). Like its related packages (‘changepoint’ and ‘EnvCpt’) a “pruned exact linear time” algorithm (Killick et al. 2012) was used as a search function with an mBIC penalty which was supervised ultimately through the “changepoints for a range of penalties” algorithm (Haynes et al. 2017a). Only one of these three packages was used for a time series at a time, depending on the state of the data. Mostly the ‘changepoint.np’ package was used since the distribution of the time series was often nonparametric. When this non-normality could be attributed to strong autocorrelation, the ‘EnvCpt’ package was used and when no autocorrelation was present and the data normally distributed, the ‘changepoint’ package was used.

The ‘bcpa’ package (Gurarie 2014), also used in a similar approach in Rust et al. (2018), was used because of its ability to compute and consider autocorrelation in incomplete time series. It uses a “window sweep” search function where a window is passed over a data series while a maximum likelihood-based cost function identifies the best changepoint locations at each step of the sweep (Gurarie et al. 2009). As a penalty term, the BIC was used. Lastly, the ‘strucchange’ package (Zeileis et al. 2002) served as a robust control because of its use in a wide range of situations. A change in regression models, in this case, a simple mean, is computed through the minimalization of the residual sum of squares (after Bai and Perron, 2003) and included through a BIC penalty, while the algorithm looks through all possible combinations of changepoints to identify the best combination (Kleiber et al. 2002). As this is computationally unfeasible a minimal limit for the segment length, i.e., the number of data points that are between the changepoints was introduced at 15% of the time series length so only the most significant changepoints were detected.

3.4 Logistic regression

3.4.1 Logistic regression predictor variables

In preparation for the regression analysis, data for possible predictor variables was compiled, analyzed, and processed. The predictors used to possibly explain a change in post-fire water quality are listed in Table 3.2. They can be divided into wildfire; watershed; reservoir; and climate characteristics. Possible predictor variables were chosen following literature review as established influencers of water quality and through their appearance in similar earlier studies or in the case of the Index of connectivity (IC) as a novel approach (Smith et al. 2011, Khatri and Tyagi 2015, Mosley 2015, Hallema et al. 2018, Rust et al. 2019). Some predictors used in other studies could not be used here because of the lack of data (e.g., soil characteristics) or focus on other variables (e.g., topographic features that are substituted partly through IC). The IC is used to closely represent areas with great soil erosion susceptibility. The characteristics were calculated for either a wildfire, reservoir, or watershed and then converted to a single value per wildfire event. Further explanation of where predictors are obtained from and how values for the regression analysis were computed can be found in Appendix A.3 Origin and calculation of regression analysis predictor variables.

Table 3.2: Characteristics that could influence a response of the water quality parameters. SPI12 is referring to the standardized precipitation index with a 12-month accumulation period, BAR to the burned area ratio, and IC to the index of connectivity.

	Predictor	Value included in logistic regression	Calculation/Source
Fire-based characteristics	Fire size	BAR	Yearly burned area clipped to watersheds / Instituto da Conservação da Natureza e das Florestas 2022)
	Fire severity	BAR with \geq low severity	Yearly burned area with Δ normalized burn ratio ≥ 0.27 ; ≥ 0.44 ; ≥ 0.66 for low; moderate; and high severity clipped to watersheds / FRISCO
		BAR with \geq moderate severity	
		BAR with \geq high severity	
Fire- and watershed-based characteristics	Sediment connectivity	75th percentile of IC maps after a wildfire season	75 th percentile of post-fire IC maps calculated after Borselli et al. (2008) / FRISCO
	Land use	BAR of Eucalyptus	Yearly burned area of a land use class as defined by the Cartografia de Uso e Ocupação do Solo 1995, clipped to watersheds / Direção-Geral do Território 2018)
		BAR of broadleaf forests	
		BAR of coniferous forests	
		BAR of shrubland	
		BAR of pastures	

Watershed-based characteristics	Watershed-area-to-volume ratio	The ratio between watershed area and reservoir volume at full capacity	Watershed area divided by the reservoir capacity / SNIRH (reservoir volumes); own calculations (watershed areas)
	Aridity	Mean aridity index (2000-2010) of watershed	Mean aridity of a watershed / Instituto da Conservação da Natureza e das Florestas 2004)
Climatic characteristics	Precipitation deviation	SPI12 of the watershed in the hydrological year before the fire	SPI12 raster map of October 1st clipped to the watershed. Mean value taken. / Global Drought Observatory (McKee et al. 1993)
		SPI12 of the watershed in the hydrological year of the fire	
		SPI12 of the watershed in the hydrological year after the fire	
Reservoir characteristics	Reservoir level	Mean reservoir level of the pre-fire hydrological year	The last value of each month was collected and the mean for a year (Oct-Sep) was calculated. / SNIRH
		Mean reservoir level of the fire year (hydrological)	
		Mean reservoir level of the post-fire hydrological year	
		Mean reservoir level of the hydrological year two years after the fire	

3.4.2 Data and variable preparation for logistic regression

The preparation of data for modeling mostly concerns the predictors, which were imputed, transformed, and standardized to meet the modeling assumptions. The occurrence of change points in the water quality parameters was transformed into binary code. Multiple imputation was done because not all predictor and response variables were complete for all data points. Multiple imputation is a procedure where missing information in one variable is estimated using covariates i.e., regressing missing cases from non-missing covariates. Generally, multiple imputation is recommended and more effective in reducing bias or elevating statistical power compared to complete-case analysis (Enders 2013), even in situations with moderate to high proportions of missing data (Madley-Dowd et al. 2019). In the case of this work, the power of the analysis would have been reduced and some predictors would have been impossible to include if only complete-case analysis would have been used. Multiple imputation of chained equations was used in this work via the ‘Mice’ R package (van Buuren and Groothuis-Oudshoorn 2011). An

overview of the fractions of missing data and the proportion of missingness before imputation is given in Table AT.1 and Table AT.2 in Appendix A.4 Missing data before multiple imputation in the predictor and response variables. The continuous covariates were imputed via predictive mean matching while binary variables were imputed through logistic regression.

After imputation, the data was transformed and standardized to represent a normal distribution as closely as possible. The variables were transformed using different transformation functions according to the best outcome fit to normality using the ‘bestNormalize’ R package (Peterson 2021). When original skewness values were between +/- 2 the variable was only scaled and not transformed.

3.4.3 Model Building

For the regression analysis, GAMs were used. The goal was to establish a regressive relation between the fire; climate; watershed; and reservoir characteristics and whether a wildfire resulted in a change or not. A different model was fitted for each of the analyzed water quality parameters. Only the qualitative effect, meaning the presence of a changepoint in a parameter was considered so logistical regression was used. The quantitative differences between changepoints are likely too complex to include in such a model (e.g., comparability of watersheds, zero inflation for non-effects, etc.).

As a first step in the model-building process, collinearity between predictor variables was assessed using principal components analysis (PCA) with the ‘vegan’ R package (Oksanen et al. 2020) and cluster analysis (through the ‘Hmisc’ R package Harrell Jr. 2022). A threshold for the correlation coefficient $|r|$ was set to 0.5 as the maximum allowed correlation between predictors (Dormann et al. 2013). Clusters of covariates with correlations above that threshold were represented through only the best fitting predictor of this cluster. The models were fitted using the ‘mgcv’ R package (Wood 2011). Parameter selection and estimation was done through a double penalization of the fitted regression splines. A penalty was added to the estimated functions to decrease their degree of freedom (“wiggleness”) and therefore avoid overfitting. Also, the null space, so the linear effects of these functions was penalized, bringing the possibility to shrink effects out of the model (Marra and Wood 2011). Penalization is used in models to stabilize their results i.e., make them less dependent on the train data, by reducing effect sizes and degrees of freedom. This approach helps to identify more significant parameter effects on the models while also making the models less sensitive to changes in these parameters than unpenalized models. All predictors with effects on the outcome were included in the final models even if p-values didn’t suggest significance, while predictors with no effects were cut from the final models. Further, no interaction terms were introduced into the final model as interactions would generally need a much higher number of samples to retrieve results with statistical power (Leon and Heo 2009). This is not saying however that interactions between predictors couldn’t play a significant role, more so they are likely to have impacts because of the underlying complexity of the processes involved especially since watershed-related variables need to interact with the wildfires to be seen. After fitting the model, predictions were calibrated using shape-constrained additive models (Pya and Wood 2015) to correct for probabilities and therefore more accurately show the effects of the predictors (Dormann 2020).

3.4.4 Model evaluation

Model performance was mainly assessed and compared through the goodness-of-fit, AIC, and cross-validated area under the curve (AUC) and root-mean-square-error (RMSE). For the goodness of fit, the explained deviance (in % of total deviance) is reported from the initial fit of the models, while the root-mean-square-error (RMSE) was computed for every test set of the cross-validation (CV). Explained deviance numbers in statistical models have a large range depending on the field of study, however in SDM values often range between 30-70% (Zurell et al. 2009, Young and Carr 2015), so values above 70% can be classified as good while values below 30% are seen as bad in this work. The RMSE was

reported to be able to compare the models with each other and can also be used to compare their performance against other logistic regression models. As a further quality metric, the area under the receiver operator characteristics curve (AUC) was taken to explain the ability of the models to correctly separate positive from negative outcomes. Cross-validated AUC is often used to determine the predictive capabilities of a model (e.g., in Zipkin et al. 2012, Durand et al. 2018, Sahin 2020) as it signals how well a model can distinguish positives from negatives in data it wasn't trained on. For this work, the classification used in El Khouli et al. (2009) was used to determine if AUC scores were good or not.

To compare the different models that had to be built because of the correlation issues between predictors AIC was used. The chosen CV method was stratified k -fold CV with k being either 5 or 10 depending on the number of positive responses. This method divides the data into k training and test sets and so assesses the performance of the models on data it wasn't trained on. 10-fold CV was favored over 5-fold CV because of its general use and suggested better performance in the literature (Marcot and Hanea 2021), however, since some parameters showed less than 10 positive results 5-fold CV was used in these cases to avoid having only negatives in a test set. Furthermore, possible violations of assumptions were checked through residual analysis of simulated residuals.

4 Results

4.1 Burned areas in the study period

Overall, 119 events in 66 reservoirs were analyzed. The BAR ranged from 0-87% for the chosen reservoirs in the study period. The biggest wildfires in terms of BAR that were suitable for analysis were in the Penedo Redondo watershed (2017: 87.4 BAR), the Bravura watershed (2003: 81.3% BAR), and the watershed of Vila Cha (2017: 69.4% BAR). The mean of the BAR for the wildfires chosen for analysis was 13.1% of the total watershed area while the median was 5.2%, so most wildfires were relatively small (<10% BAR) with lesser medium-sized wildfires (10-50% BAR) and just a few big wildfires (>50% BAR).

4.2 Change point analysis

The results for all parameters and reservoir stations of the CPA can be found in Table AT.3 in Appendix A.6 Results of the change point analysis. The number of change points, and the positive ratio, meaning the ratio of CPs through all observations can be seen in Table 4.1. The positive ratio ranges from 5 to 22%. COND is by far the parameter with the most CPs and highest positive ratio, while BOD, COD, DO and pH all have low positive ratios of around 5-7%. COD has a higher positive ratio than BOD even though the number of CPs is the same because of the higher number of NAs (12 vs. 4 for BOD). During the CPs of DO, the concentration decreased two times while raising four times, while pH decreased during four out of eight times CPs. In the water quality parameters of COND and P, there were two, respectively one CPs that lead to decreases. These were however not considered in the models later on as only increases are reported in the literature (Smith et al. 2011).

Table 4.1 Number of CPs per parameter and the CP ratio for the biological oxygen demand (BOD), chemical oxygen demand (COD), conductivity (COND), total phosphorus (TP), nitrate (NO₃), dissolved oxygen (DO), total suspended sediments (TSS), and pH.

Parameter	CPS	Positive Ratio (%)
BOD	6	5.2
COD	6	5.6
COND	26	21.8
TP	11	9.6
NO₃	15	12.6
DO	6	5.1
TSS	16	13.6
pH	8	6.8

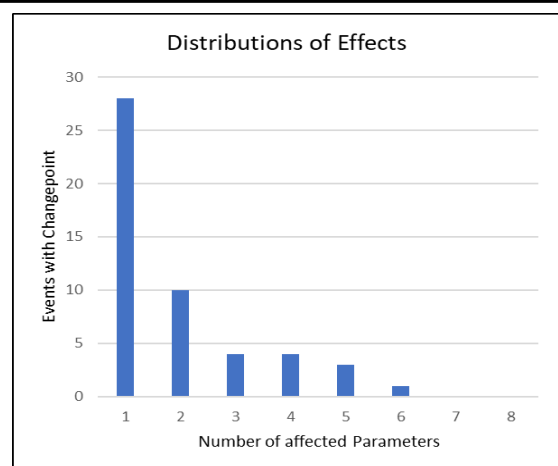


Figure 4.1: Distribution of the number of affected parameters per wildfire event.

At least one parameter experienced a CP in over 40% of total cases. No events had CPs in seven or all eight parameters and 69 out of the 119 events had no change points in any of the parameters (Figure 4.1). The exponential declining shape of Figure 4.1 suggests no extreme patterns of correlations between response variables. This is supported by an analysis of pairwise correlations and clusters in the response variables where moderate correlations (according to Cohen 2013) were found between some of the parameter CPs. A slight cluster of similar effects can be found between TP, NO₃, COD, and TSS as well as between COND and pH (Figure 4.2), suggesting that e.g., TSS, nutrients, and COD show similar effects. Pairwise phi-coefficient correlations, which for dichotomous variables represent the Pearson

correlation coefficient (Ekström 2011), however, were all below 0.5 (below 0.25 in Figure 4.2 as correlations are squared).

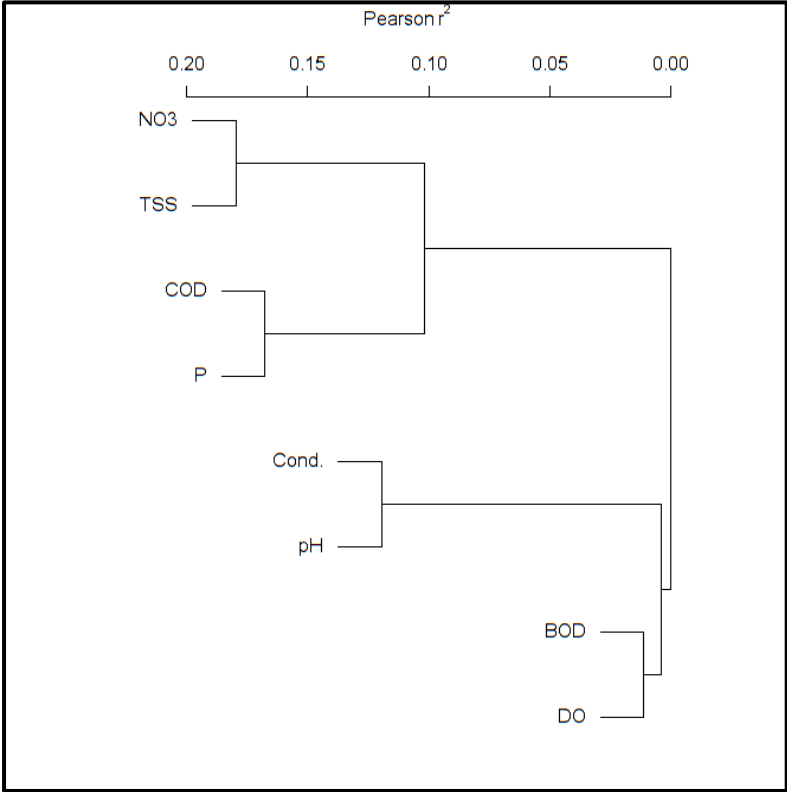


Figure 4.2: Cluster analysis of the response variables biological oxygen demand (BOD), chemical oxygen demand (COD), conductivity (Cond.), total phosphorus (TP), nitrate (NO3), dissolved oxygen (DO), total suspended sediments (TSS), and pH. Values are given in squared Pearson correlation, which represents the squared phi coefficient for binary variables.

4.2.1 Spatial and temporal distribution of effects

To identify possible hotspots of post-fire water contamination, maps of the water quality parameters and their affected watersheds are displayed in Figure 4.3 and in further detail in Figure 4.4.

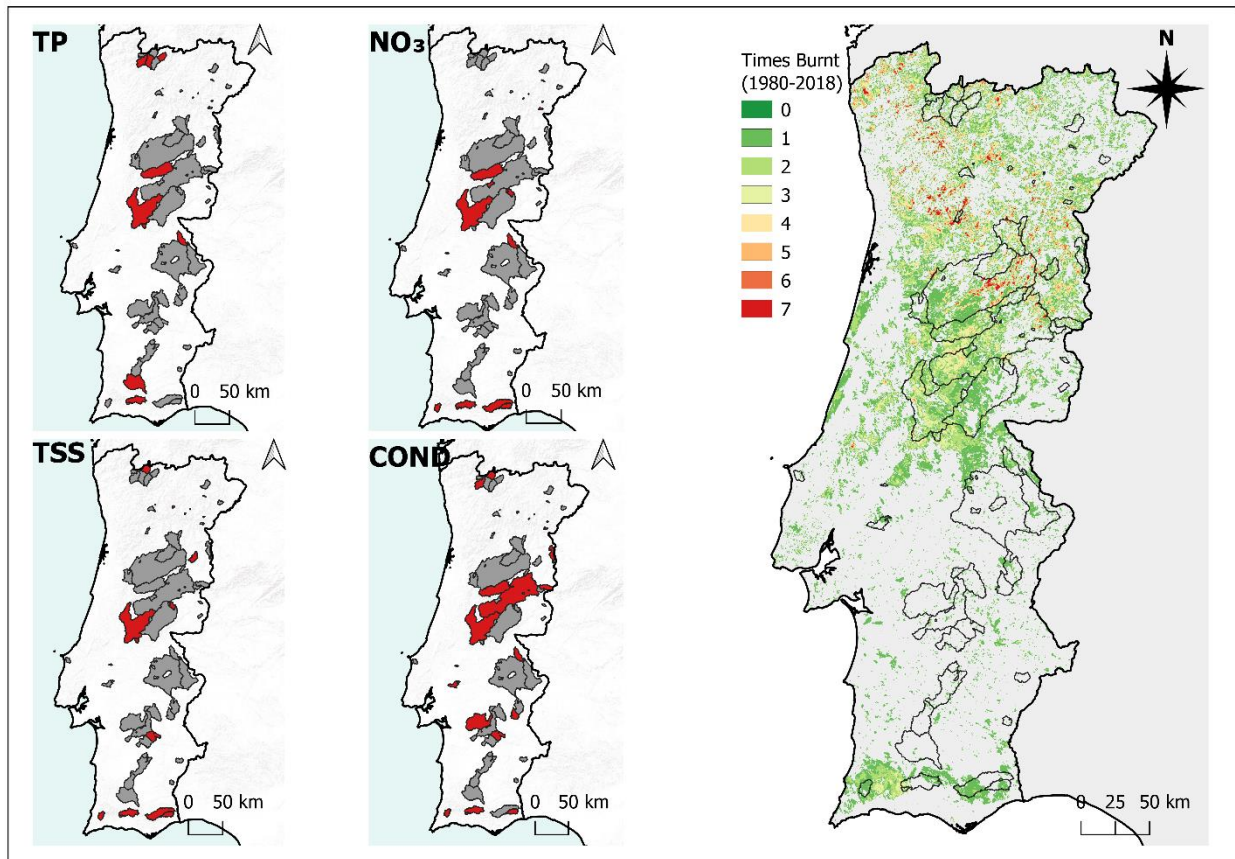


Figure 4.3: Affected reservoirs (represented through their watersheds) for the parameters of total phosphorus (TP), nitrate (NO₃), total suspended sediments (TSS), and conductivity (COND), where red colour indicates a changepoint and grey colour indicates no changepoint in the watershed for any wildfire event. The map on the right displays the number of times that an area was burnt (from 1980-2018), as a direct visual comparison between reservoir impacts and burnt areas.

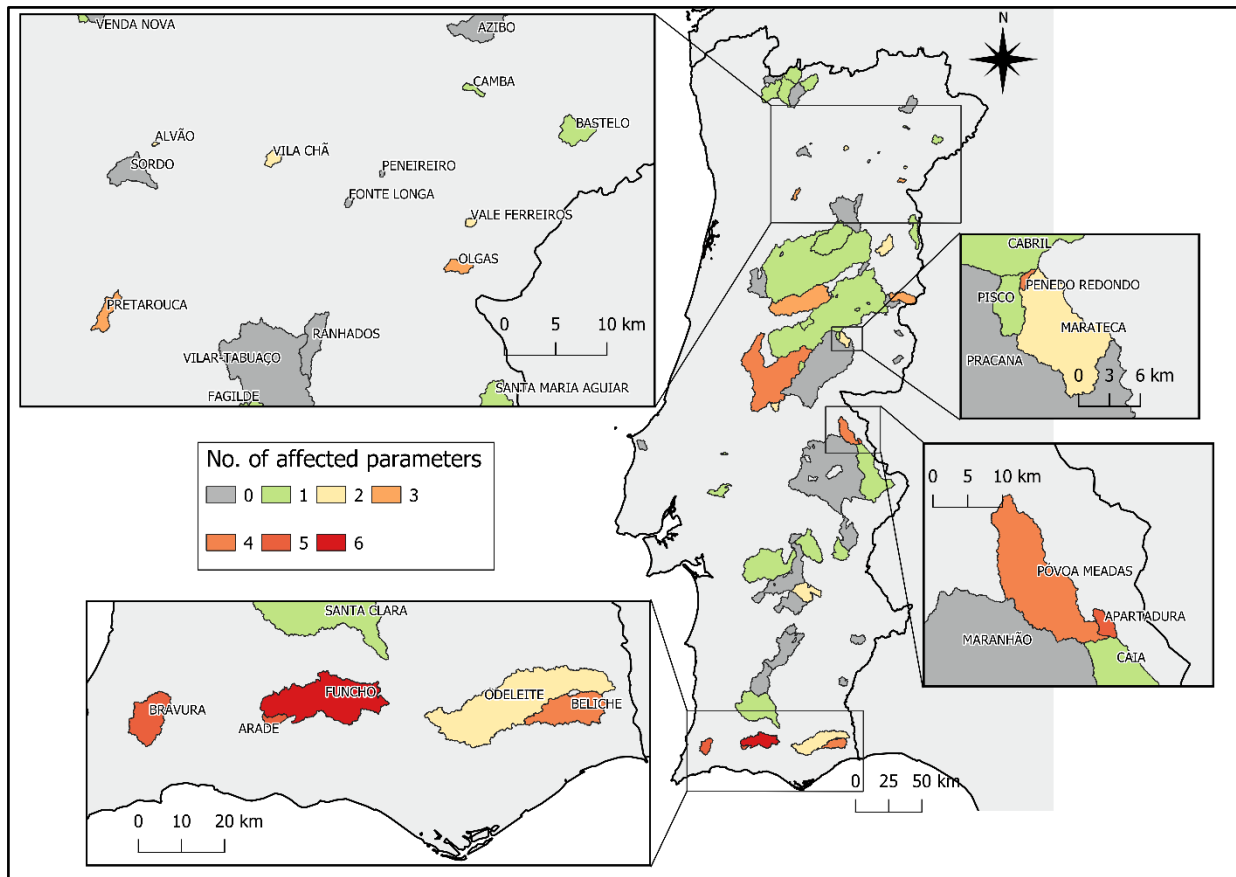


Figure 4.4: Detailed map of the number of affected parameters per reservoir (represented through their watersheds) in the most impactful fire event. Visible is a cluster in the south and spread throughout Central and northern Central Portugal.

TSS and NO_3 show similar spatial patterns which also seem to visibly correlate with fire recurrence in Portugal (Figure 4.3). In both parameters, the watersheds of the Algarve are all affected while a second cluster of effects can be found in the central region. For TP and COND, on the other hand, effects are more evenly distributed. TP has affected watersheds in the far south, the central mountainous terrain, and the far north, while COND has affected watersheds in nearly every region. The spatial distribution of the number of affected parameters for a single wildfire event follows the spatial distributions of NO_3 and TSS more closely. All watersheds in the Algarve have at least two affected parameters, while three of the four most affected watersheds can be found in the area (Bravura, Arade, and Funcho). The second most affected area is the center of Portugal where a few watersheds with more than one affected parameter are located e.g., near Coimbra and near the Serra de São Mamede natural park, in mountainous terrain (Figure 4.4).

Not only could effects be clustered in space, but they also show differences in time. In the study period, the BA oscillated around 100 000 ha of BA each year, while years with higher area burnt were normally followed by years with less area burnt. Two major exceptions are the wildfire seasons in 2003-2005 and 2017, wherein the former over two times and in the latter over four times more area was burnt yearly than the 1985-2018 average (Figure 4.5).

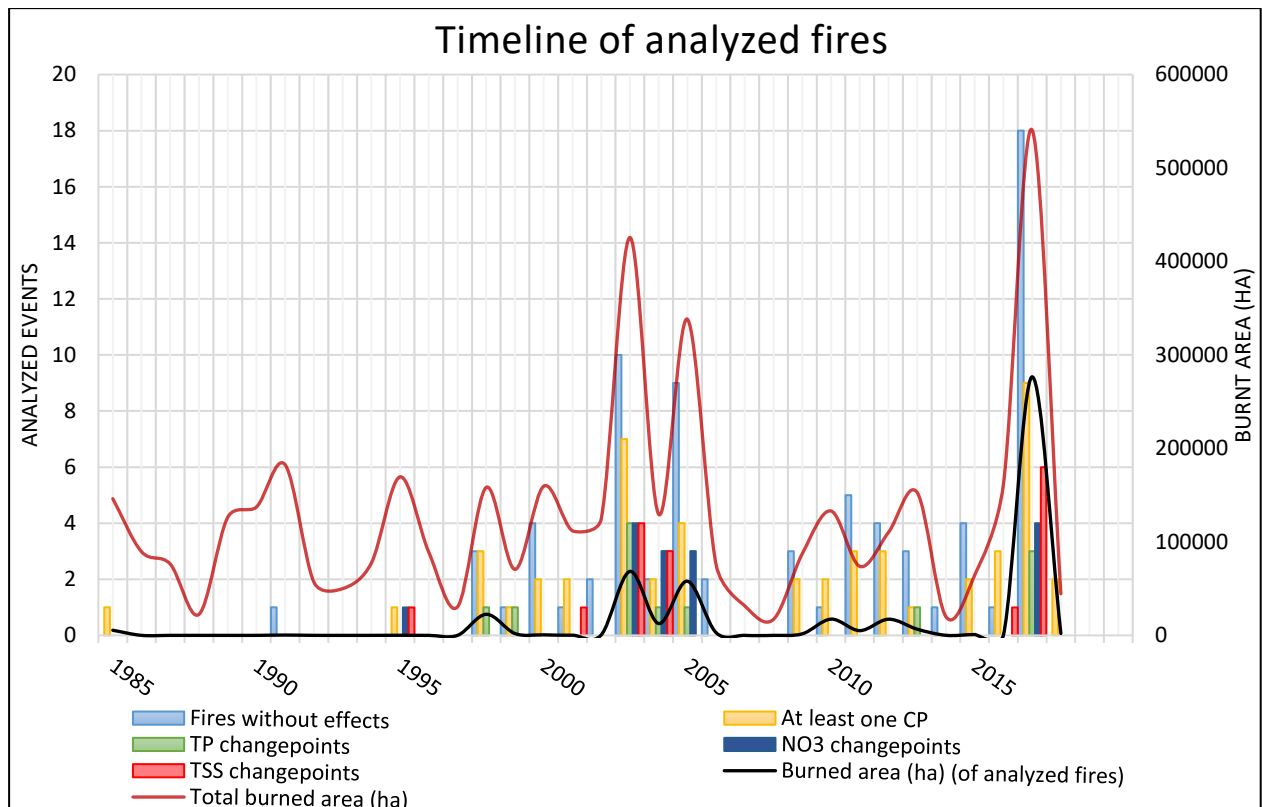


Figure 4.5: Timeline of analyzed wildfires and events with changepoints in certain WQ parameters. The number of watersheds with no effects (light blue) and with at least one CP (yellow) is also shown, as well as the total BA of Portugal (red line) and the total BA of the analyzed events (black line).

In most years there are more events without CPs than there are events with at least one CP. The chosen events mostly represent between 5–20 % of the total BA each year except for 2017, which is overrepresented in terms of BA (~50% of total BA covered), and the period before 1998, which is underrepresented. The CPs of TP, NO₃, and TSS are concentrated in the major wildfire seasons of 2003-2005 and 2017. This is in slight contrast to the other parameters which are more evenly distributed.

Further, all wildfires where four or more parameters were changing for a single event are between 2003 and 2005 except for Penedo Redondo (2017: 87% BAR), where four parameters showed a CP. This could point towards either more overall effects in that wildfire season or a general vulnerability of the Algarve region, where the biggest wildfires were happening in those years. The wildfire season of 2017 had major fires (with BARs of >30%), where only little to know effects were present in the watersheds of Central Portugal. Here the big reservoirs of Aguieira, Cabril, and Castelo de Bode stand out which have a combined area of over 608 000 ha of which 44%, 25%, and 33% burned respectively, while only elevated NO₃ levels were seen in Castelo de Bode and elevated COND in Cabril.

4.2.2 Quantitative analysis of TSS changepoints

Only the parameter TSS was investigated with more detail, as it was identified as a risk parameter for water supply by FRISCO partners, and quantifying effects for all parameters is beyond the scope of this work. Of 16 CPs that were detected through the CPA, all surpassed a threshold of 5 mg/l above which water supply could be disrupted (Langhans et al. 2016). In some stations, maximum concentrations of 599 mg/l (Arade, 2005) and 188 mg/l (Funcho, 2005) were measured.

The 5 mg/l threshold value is however and most likely based on a 5 NTU (Nephelometric Turbidity Unit) turbidity limit recommendation that was brought forward by the World Health Organization as the

lowest acceptable threshold for water supply (World Health Organization 2011). These two parameters, although they are often found to be highly correlated (e.g., Holliday et al. 2001, Rügner et al. 2013) cannot be used interchangeably, so a 5 mg/l threshold should be handled with care. Nonetheless, high TSS values can still pose a serious threat to water supply, especially if there are no or not sufficient pre-treatment stations present. Even if there are, higher TSS concentrations increase operational costs for e.g., disinfection, coagulation, and flocculation (Bladon et al. 2014, Martin 2016).

Moreover, the properties of the TSS CPs were compared for the two major wildfire seasons (2003-2005 and 2017). The goal hereby was to also gain a quantitative perspective of water quality changes. The deviation from the mean TSS concentration as well as the length of the CPs was compared. Differences can be seen in the boxplots below (Figure 4.6).

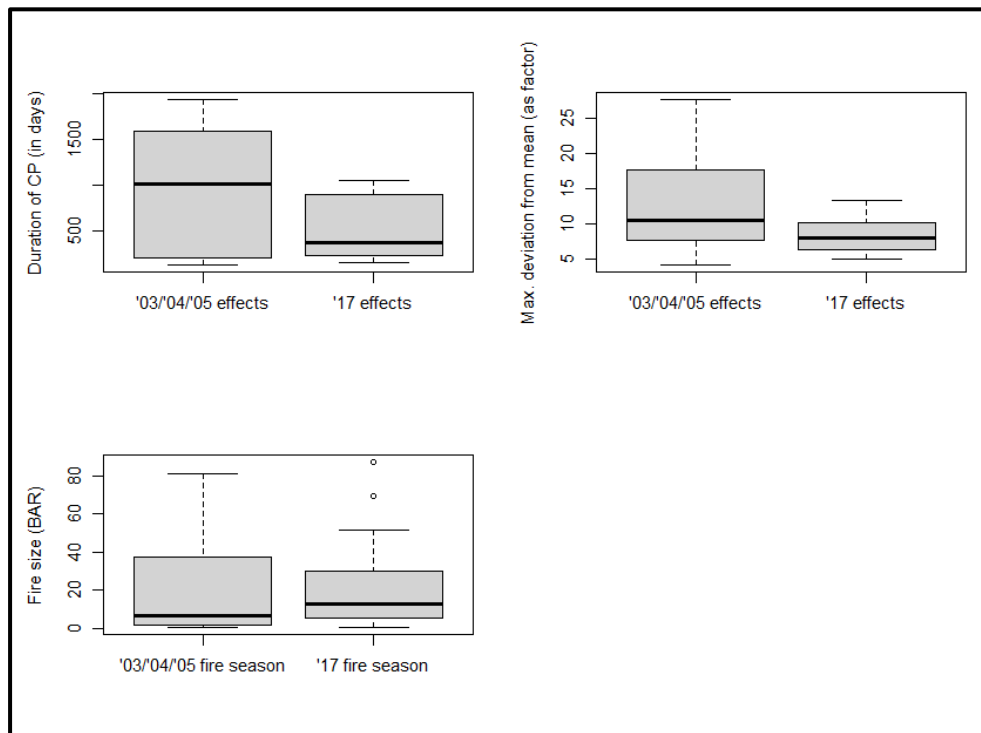


Figure 4.6: Boxplots of the duration of the changepoints (CPs), compared across the two major wildfire seasons (top left), the deviation of the highest measured concentration inside the CP range as a factor of the overall mean over the time series (top right) and the burned area ratio (BAR) of the analyzed events (so independent from CP or no CP) from both wildfire seasons (bottom left).

The wildfires in the 2003-2005 season, had overall longer and “stronger” effects than the 2017 wildfire season, with the deviation from the overall mean of the respective time series being greater in the 2003-05 wildfire season than in 2017 (Figure 4.6). Also, the average duration of a CP was slightly longer after the 2003-2005 wildfire season compared to 2017 (Figure 4.6). The average BAR was slightly higher in 2017 (21% BAR vs. 18% BAR in 2003-2005). Overall, fire sizes are similar in both periods.

It should also be stated that the end of a changepoint is possibly harder to identify than its start since a start is marked by a pointwise disruption of the system (a wildfire) which can have a sudden impact while the end of a changepoint can be a point in the steady process of normalization and vegetation regrowth and might not always be identified correctly by the used methodology.

4.3 Modelling results

Due to correlations in the predictor variables over the set threshold ($|r| \geq 0.5$) some of the predictors could not be used simultaneously (see Figure AF.2 in Appendix A.5 PCA and Cluster analysis of

predictors:). A high correlation between covariates was found within the reservoir level predictors (pre-fire-year reservoir level, fire-year reservoir level, post-fire year reservoir level, 2-years-post-fire reservoir level), between fire-year, and post-fire-year SPI12, and within a cluster including fire size, all fire severity predictors, the IC, and the land use predictors of shrub and coniferous forests. The reservoir level cluster was represented through the post-fire-year reservoir level, as this was always the best-performing predictor within this cluster. The same applied to the SPI, where the fire-year SPI12 was taken to represent these two predictors. To compare predictor performances of the covariates found in the fire size cluster (fire size, fire severities, IC, shrub, coniferous forest) a fire size based (FSB) model, with all other uncorrelated predictors, was compared against a severity-based (SB) model, which included the best fitting fire severity predictor (\geq low severity; \geq medium severity, or \geq high severity) and the IC predictor as well as all other uncorrelated predictors. Shrub and coniferous forests did not improve the models in any case and are therefore not used. Model evaluation scores of the distinct models with the best combination of predictors can be found in Table 4.2.

Table 4.2: Model evaluation scores for the parameter models. The area under the curve (AUC) and root-mean-squared error (RMSE) are based on either 5-fold or 10-fold stratified cross-validation of the calibrated models. Good deviance explained and AUC values are highlighted in bold. Akaike Information Criterion (AIC) and RMSE are seen as comparative quality metrics. Reported are the scores for the fire size-based (FSB) and severity-based (SB) models for the parameters biological oxygen demand (BOD), chemical oxygen demand (COD), conductivity (COND), total phosphorous (TP), nitrate (NO₃), dissolved oxygen (DO), total suspended sediments (TSS), and pH.

Models	Deviance explained (in %)	AIC	AUC	RMSE
BOD FSB	49.4	41.8	0.827	0.243
BOD SB	72.5	38.3	0.743	0.303
COD FSB	26.9	54.9	0.795	0.244
COD SB	25.7	55.5	0.777	0.292
COND FSB	38.6	108.6	0.663	0.465
COND SB	40.2	106.5	0.679	0.460
TP FSB	28.5	63.8	0.917	0.247
TP SB	38.8	63.6	0.844	0.300
NO₃ FSB	49.4	55.8	0.900	0.241
NO₃ SB	65.3	54.1	0.857	0.297
DO FSB	54.6	41.6	0.629	0.271
DO SB	73.0	35.7	0.624	0.334
TSS FSB	46.1	68.1	0.870	0.295
TSS SB	37.5	77.8	0.816	0.385
pH FSB	26.8	52.0	0.716	0.257

pH SB	28.2	55.3	0.761	0.287
--------------	------	------	-------	-------

All BOD models explained a fair amount of deviance, but the better fitting SB model had worse cross-validated AUC and RMSE scores, while the FSB model had good AUC scores according to El Khouli et al. (2009). A good initial model fit with bad CV performances could indicate overfitting or similar problems, because of which the FSB model is preferred here. The models for COD had less explained deviance than the BOD models with average AUC values. This time the fire size-based model outperformed the severity-based model in the initial model fit while performing slightly worse on CV AUC scores. The differences between the models were however marginal. AUC and RMSE scores for the COND models were the worst out of all modeled parameters. The SB model outperformed the FSB model slightly in all evaluations. While the initial model didn't result in a severely bad fit, the poor performance during CV indicates bad predictive power and performance.

The SB TP model explained more deviation than the FSB TP model, but AIC scores were almost identical since the FSB used fewer parameters for the regression. Together with CV AUC and RMSE values, the FSB model seems to outperform the SB model. Overall, both models showed good to excellent predictive powers, with the FSB TP model having the best AUC across all models. NO₃ showed a preference for the fire size-based model. The FSB model was fitted with a manually penalized smooth for pasture as the effects suggested an overfit for that parameter which resulted in an increase in AUC scores to 0.9. The new fit also shrunk down the differences in performance between the FSB and SB models with the SB model having a slightly better AIC. In CV both models are very similar with good AUC and RMSE values, while the FSB model outperforms the SB model.

DO models are reported, while having in mind that only six CPs were present, with two decreases and four increases. Still, explained deviances of both models are high. The SB model is preferred by explained deviance and AIC. The AUC for both models is slightly above 0.6 after calibration, pointing towards low discriminative power. This indicates that the parameter might not be ideally modeled with the available predictors.

The TSS models performed relatively well in the evaluation of the initial fit and through CV, compared to the other parameter models. The FSB model was preferred by AIC and explained deviance. AUC scores were above 0.8 for both models (Table 4.2), indicating good predictive capabilities and the RMSE was also low. In the initial fit, the FSB model performed better than the SB, while differences across CV were slightly lower. Overall, the FSB model outperformed the SB model.

PH overall didn't show a good performance. The FSB model was preferred by AIC while in CV the AUC for the SB model was slightly higher (Table 4.2). Neither model reached good AUC scores. RMSE scores of the pH models are again better for the FSB model, so overall neither of the models is ideal to explain or predict the CPs.

4.4 Most important model predictor effects

This sub-chapter reports the most consistent and influential predictors i.e., the predictors that showed similar effects across the range of the different parameter models and that were responsible for the largest parts of explained deviation. A predictor that induces similar effects over a range of different models is more likely to have a "true" impact on these parameters. Other predictors that were only chosen for single models or were highly variable will be named at the end of this sub-chapter.

4.4.1 Fire size

The most consistent and influential predictor overall was fire size, which showed effects for six out of eight models for the different parameters. In five of these cases, the p-value for an effect was below the 5% significance threshold (COND, TP, NO₃, TSS, and pH). The effects can be seen in Figure 4.7. The effects are very consistent across the different models with an increase in fire size translating to an increase in the probability of a CP. An exception is the effect in TSS where also very low fire sizes induced an increase in CP probability. The effects were generally linear with some, especially TSS, being almost exponential. The effect sizes varied across the parameters, so e.g., for the case of TSS, a BAR of 50% meant a high probability of experiencing a CP (>90%). The predictor had fewer effects on COD, COND, and pH, where even fire sizes of 75% BAR only resulted in a <25% chance of experiencing a CP when all other values were at their mean. Models that included fire size instead of fire severity often outperformed SB models during cross-validation, while having a worse goodness-of-fit in the initial model fit. But since differences between those models were mostly slim, fire size can be seen as an overall very important predictor.

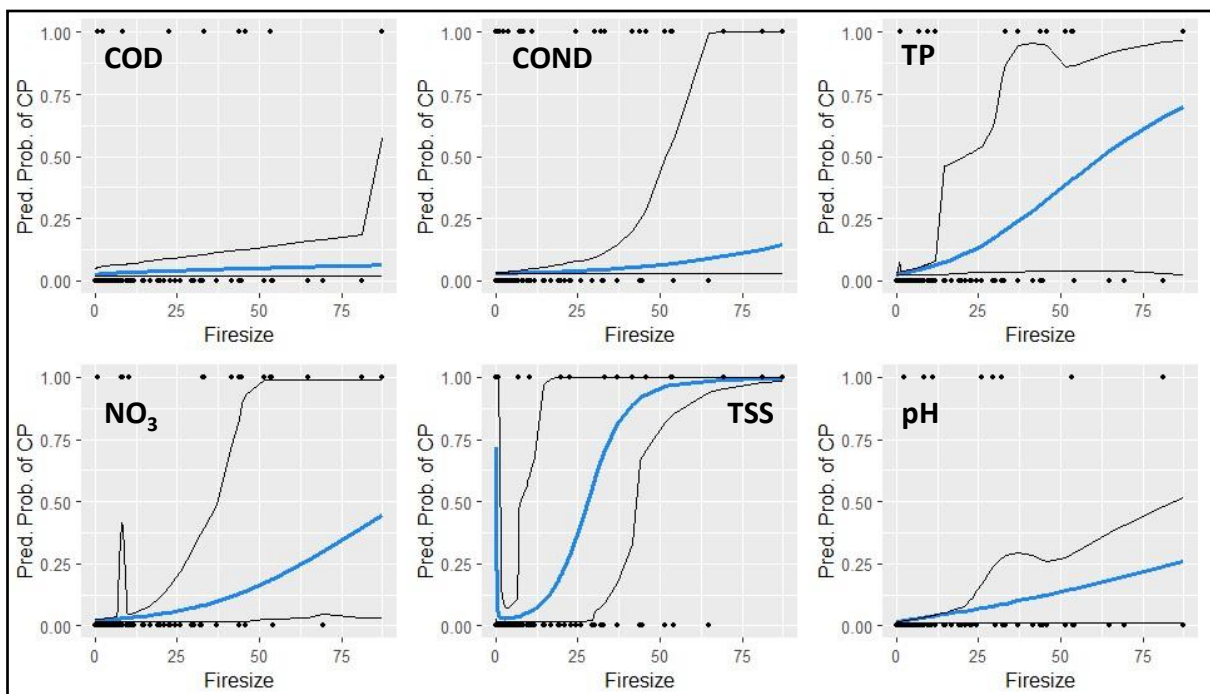


Figure 4.7: Effects of fire size on the models of biological oxygen demand (BOD), conductivity (COND), total phosphorous (TP), nitrate (NO₃), total suspended sediments (TSS), and pH. Predicted probabilities for a change are on the y-axis on a scale from 0 to 1, with one being a 100% predicted probability and the fire size on the x-axis in % BAR. The blue line represents the modeled effects. The plots were calculated by setting all other model parameters to their respective mean, to have constant effects. The black lines are confidence intervals that represent the 2.5 and 97.5 percentiles of models from bootstrapped data.

4.4.2 Fire severity

Fire severity was not represented as one predictor in the models. Instead, three different predictors were used, which were the BAR \geq low severity, the BAR \geq medium severity, and the BAR \geq high severity, all according to different Δ NBR levels. The three different categories were not used simultaneously in the models. Overall fire severity had an effect in five models, three were with a p-value of <0.05 (COND, TP, and TSS). Like fire size a general increase in the area meant an increase in the probability of a CP, but with overall fewer effects (Figure 4.8). FOR COD and DO, no increase and only marginal effects can be seen. The BAR \geq low severity was taken as the best representation of the fire severity in two models (COND and DO), while the BAR \geq medium severity was taken best pH model TP. The BAR \geq high severity was also the best fit for two models (COD and TSS). So, none of the severity classes

performed consistently better than others and total effect sizes were generally low, except for TSS. Even in this parameter the chance for a CP stayed below 50% for high values if all other predictors were at their mean.

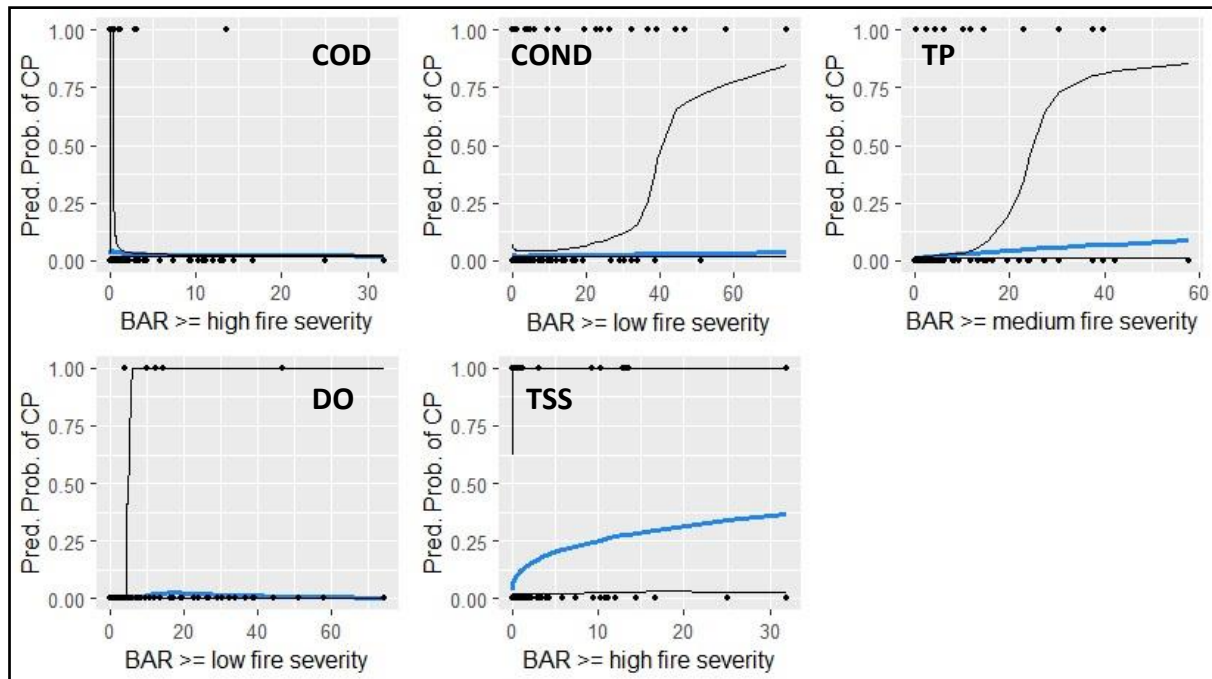


Figure 4.8: Effects of different levels of fire severity on the models of chemical oxygen demand (COD), conductivity (COND), total phosphorous (TP), dissolved oxygen (DO), and total suspended sediments (TSS). Probabilities for a change are on the y-axis on a scale from 0 to 1, with one being a 100% predicted probability and the fire severity on the x-axis in % BAR with \geq low; medium, or high fire severity, depending on which predictor resulted in the best fit. The blue line represents the modeled effects. The plots were calculated by setting all other model parameters to their respective mean, to have constant effects. The black lines are confidence intervals that represent the 2.5 and 97.5 percentiles of models from bootstrapped data.

4.4.3 Sediment connectivity

The IC was taken as a predictor which can closely represent wildfire effects on soil erosion. It was used in the SB models but could not be used in the FSB models due to the correlation of covariates. The value used to represent the IC was the 75th percentile of the post-fire watershed IC maps. As seen in Figure 4.9, most of the effects, that were caused by the predictor of fire size in the FSB models were substituted with the effects of sediment connectivity in the SB model. The results show reasonable effects of IC on the probability of a change, with seemingly large effect sizes (Figure 4.9). Problematic, however, is the presence of outliers which distorts the effect plots. This can be seen in the plots of COD, TP, NO₃, and TSS where high IC 75th percentile values (IC75) show probabilities for a change close to or even at one influenced by just one occurrence (Penedo Redondo, 2017 with an IC75 value of -5.7 and a BAR of 87.4%). In the cases of COD, NO₃, and TP, the effects before being influenced by that outlier only reach around a 25% chance of change and then jump to over 75%. This outlier also explains the sudden drop in the likelihood of a CP in the pH plot.

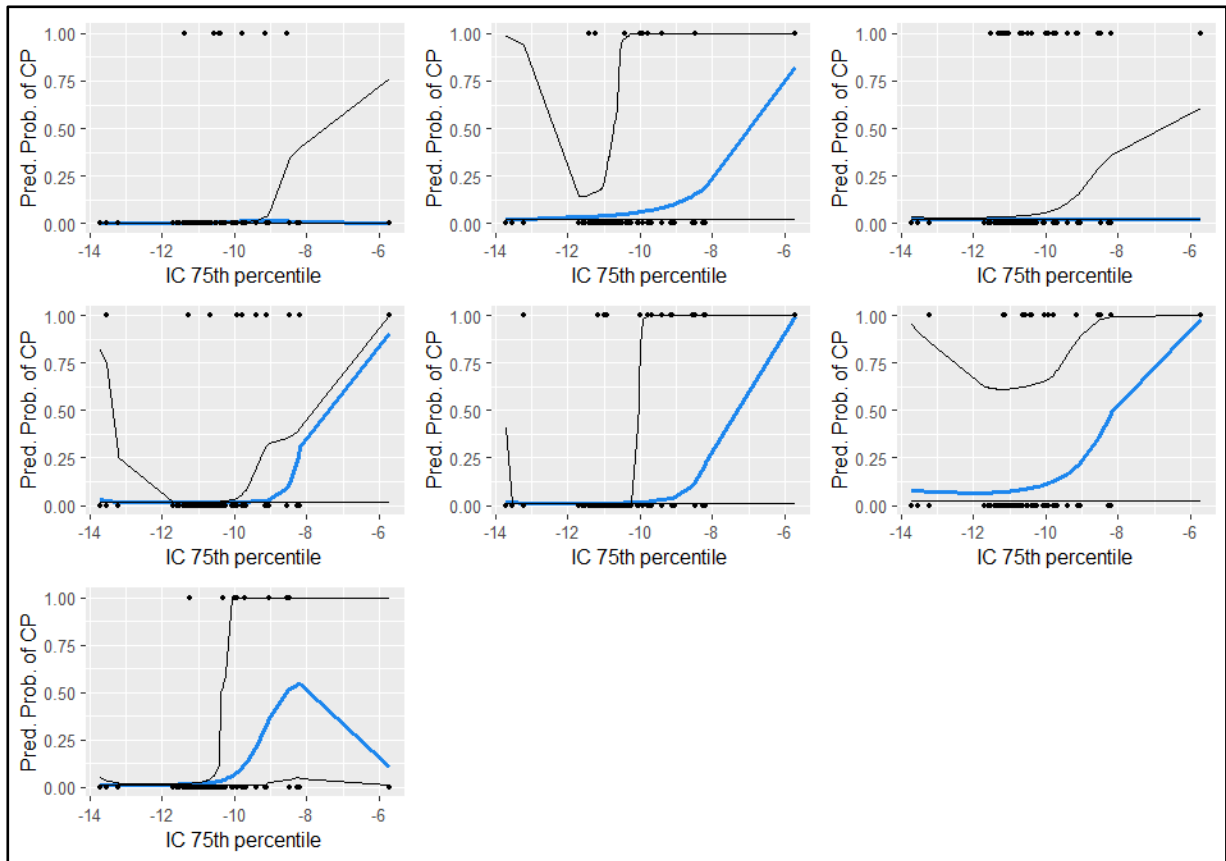


Figure 4.9: Effects of the index of connectivity (IC) as a measurement of sediment connectivity on the models of biological oxygen demand (BOD), chemical oxygen demand (COD), conductivity (COND), total phosphorous (TP), nitrate (NO₃), total suspended sediments (TSS), and pH. Probabilities for a change are on the y-axis on a scale from 0 to 1, with one being a 100% modeled probability and the IC on the x-axis represented by the 75th percentile value of the IC map in a burnt watershed. The blue line represents the modeled effects. The plots were calculated by setting all other model parameters to their respective mean, to have constant effects. The black lines are confidence intervals that represent the 2.5 and 97.5 percentiles of models from bootstrapped data.

Even though the outlier represents the largest BAR in this work and is therefore likely not just a miscalculation, it should be avoided to make assumptions about the likelihood of CPs based on just one observation. Still, with the 75th quantile for IC, the predictor showed an effect for seven out of eight models, being under the <0.05 p-value threshold for significance in five models (BOD, TP, NO₃, TSS, and pH). An increase in CP probability could be seen for increasing IC75 values, which are marking an increase in sediment connectivity, and even before being influenced by the outlier, the effect sizes are larger than the fire severity effect sizes. The results show a likely relationship between sediment connectivity and water contamination episodes.

4.4.4 Reservoir levels

Changes or differences in reservoir levels are an effect that is not directly related to the group of fire-related predictors, although low reservoir levels that are present in drought scenarios can point to a higher inflammation risk and general risk for high severity fires (Russo et al. 2017, Pausas and Keeley 2021). In this work pre-fire-year, fire-year, post-fire-year, and two-years-post-fire reservoir levels were tested individually in the models. Reservoir levels were taken based on the hydrological year. Out of the four time periods of reservoir levels, the post-fire reservoir level consistently performed best and is shown and referenced when talking about reservoir levels in this chapter (Figure 4.10). Reservoir levels had an effect in five out of eight models. three of these effects were significant based on the <5% p-value threshold (only pH and DO were not significant). As there was no strong correlation between this

predictor and fire size, severity, or any other predictors except for other periods of reservoir levels it could be included in all models. The reservoir level further showed an effect in the SB TP model, however, this effect is not shown in Figure 4.10, since that model was not chosen as the best performing TP model. The effect of the reservoir level in that model was however like the ones shown, although small. Effects were consistent with a decrease in reservoir level inducing an increase in CP probability on an exponential scale except for pH where increases resulted in a slight probability decrease. Further, the effect of the reservoir level did not change structurally between FSB and SB models for the same water quality parameters, except for DO where the reservoir level had a much bigger influence on the FSB model (up to 75% of CP at low reservoir levels). Effects also only started to become strong in scenarios of severely low levels (<0.8 or i.e., <80% of the maximum storage level).

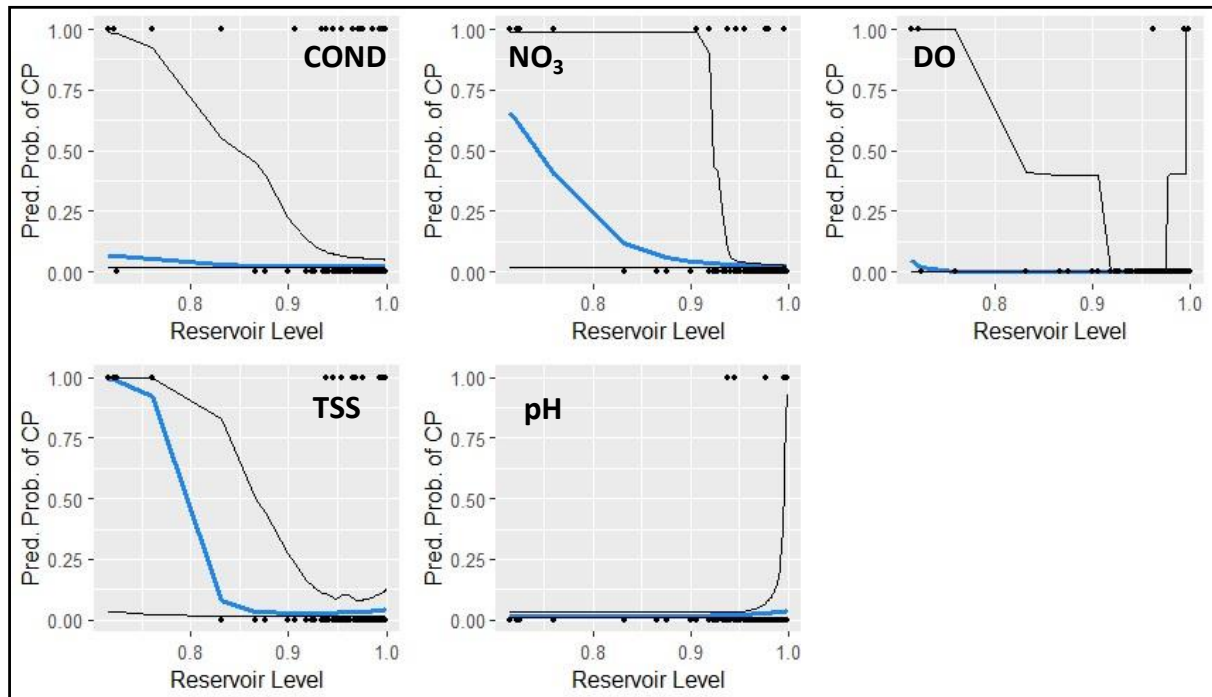


Figure 4.10: Effects of post-fire-year reservoir levels on the models of conductivity (COND), nitrate (NO₃), dissolved oxygen (DO), total suspended sediments (TSS), and pH. Predicted probabilities for a change are on the y-axis on a scale from 0 to 1, and the reservoir level on the x-axis as the storage ratio of the maximum storage level. The blue line represents the modeled effects. The plots were calculated by setting all other model parameters to their respective mean, to have constant effects. The black lines are confidence intervals that represent the 2.5 and 97.5 percentiles of models from bootstrapped data.

4.4.5 Further predictors

Further, other parameters were included regularly in the models but were either inconsistent (pre-fire-year and fire-year SPI12 and the watershed-area-to-volume ratio) or only showed minimal effects for all the models (pastures as a land use type for BAs where a general increase in probability for a CP is visible but effects, in general, are low). Still, the BAR of pastures was included in five models with similar trends, so according to the models, an effect can be seen from that characteristic. Further, predictors such as the broadleaf forest land use type, or the aridity index were only chosen in one and two models. These predictors are not presented in more detail in this sub-chapter as their general effects in the models are inconclusive or can be neglected, except for arguably the effect of pastures. A higher number of data points would maybe give a clearer picture if some of these predictors have a true effect on post-fire water quality and the inclusion of interactions into the models would especially help to identify effects that are caused by characteristics that are not directly linked to the fire itself, like the watershed-area-to-volume ratio, the aridity of the watershed or SPI measures. With that in mind, the influences of these predictors will be discussed.

5 Discussion

During this work, events of post-fire water contamination in Portuguese water reservoirs were identified from a publicly available database of time series. The use of such a database allowed for the analysis of multiple wildfires and therefore the extraction of possible drivers of post-fire water quality response in reservoirs. With this approach, this work follows up on earlier analyses conducted e.g., by Hallema et al. (2018), Saxe et al. (2018), and Rust et al. (2018). In my work, I found changes after wildfires in at least one out of the eight considered water quality parameters in over 40% of selected fires. The frequency of the responses varied greatly from parameter to parameter with 5-22% of events resulting in a changepoint after wildfires. Fire size, the index of connectivity as a measurement of sediment connectivity, and post-fire-year reservoir levels were all identified as possibly important drivers, especially for modeling nutrients (TP and NO_3) and total suspended sediments. The models could also discriminate changepoints from no reaction in those parameters better than in the other parameters given the tested predictors. With these results, the current work only partly agrees with earlier analysis, which found that fire severity plays an important role in dictating post-fire water quality response. Although fire severity was used in the models, reactions were generally represented better by using fire size. Possible reasons for this effect will be discussed. Further, this work adds to the current discussion that reservoir internal drivers, such as the reservoir level and subsequent volume play an important role in mitigating or amplifying the effects of wildfires.

5.1 Parameter responses

Noticeable in the post-fire water quality response were the different positive ratios (so the number of changepoints) across the water quality parameters. BOD, COD, and DO have the lowest positive rates of all-around 5% of all parameters. Based on their response mechanisms, these parameters would be also expected to be correlated, as COD and BOD are key factors in determining the DO. However, correlations of CPs occurring simultaneously in these parameters were small (according to Cohen 2013). BOD and COD were often parameters where the data quality of the time series was especially bad. They had high detection limits and sometimes data gaps, so the concentrations of BOD and COD were mostly below the detection limits. Post-fire reactions could therefore be made up of short spikes, that in some cases would stay under the detection limits and are not picked up as a changepoint by at least two out of three methodologies (see exemplary evidence in Figure 5.1). Even with these difficulties, model performance of BOD and COD was rather good, suggesting a relationship between the tested predictors and the oxygen demand. This is supported by the medium correlation (after Cohen 2013) between COD changepoints and TP, NO_3 , and TSS changepoints, suggesting that the reaction of COD has similarities to the reactions of TSS and the measured nutrients. With better data quality, especially lower detection limits, possibly more changepoints could have been identified.

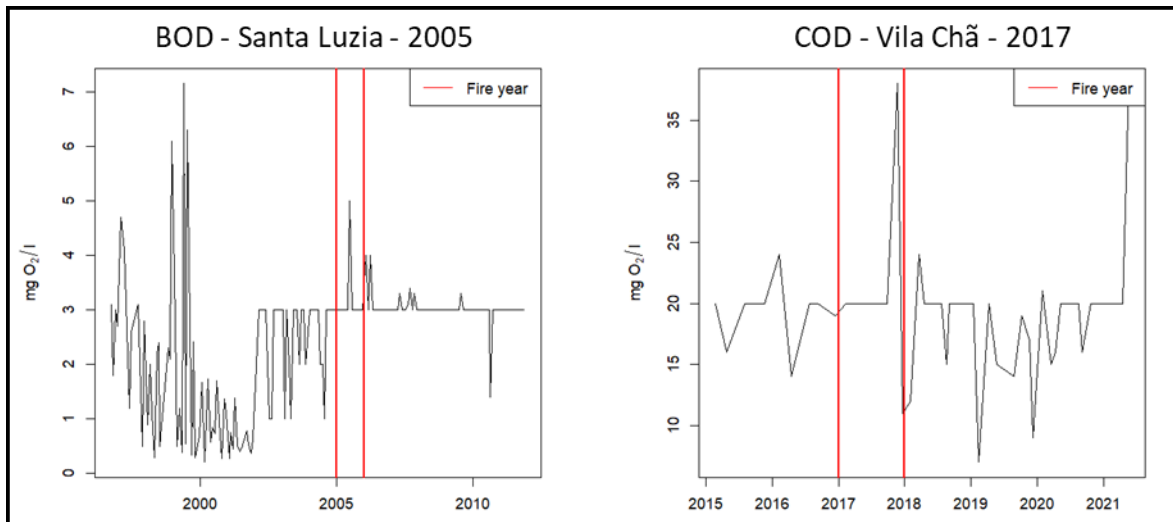


Figure 5.1: Examples of elevated post-fire biochemical oxygen demands that did not get picked up by the changepoint analysis, likely due to high detection limits and only short spikes in the parameters.

The same could not be said about DO, where almost no data was below a detection limit (<1% of data points) and sampling frequency was comparably good. However, the parameter was seldom affected after fires and even increased in four out of six occasions, which contradicts previous observations, although from rivers and headwaters (e.g. Earl and Blinn 2003, Sherson et al. 2015). This was rather surprising as DO is a parameter often reported to change, and decrease, after wildfires. The reasons for the low detection rate and counterintuitive response are most likely explained through the analysis methodology and reservoir processes. While the introduction of sediments and ashes should instantly reduce DO based on their chemically reducing properties, the introduction of nutrients acts as a fertilizer in the reservoirs. This enhances primary production and therefore photosynthesis and respiration, which causes higher daytime concentration maxima but also lower nighttime concentration minima (Reale et al. 2015). As DO levels are measured throughout daytime in the available time series, levels are increased through active photosynthesis which leads to DO oversaturation. Further, the high variance in the DO time series might also explain why so few changes were picked up during the CPA. Changes in concentration would have to be high or present over a long period for the CPA to recognize them.

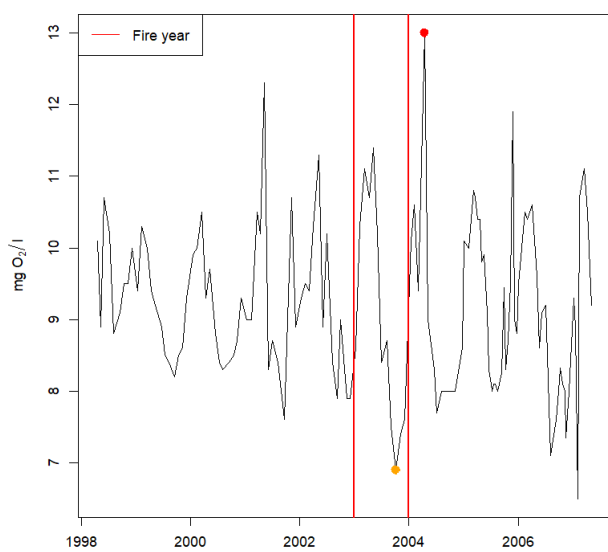


Figure 5.2: DO concentrations in the Bravura reservoir from 1998-2008. The red lines mark the 2003 fire year, while the orange point marks a local minimum and the red point a global maximum.

Yearly DO levels often seasonally oscillated around 6 to 12 mg/l in the data, with high values in winter and low values in summer and fall, while fires caused short-term increases that were too small to be significant. One example is the Bravura watershed, which burned over 80% in 2003. Shortly after the fire DO levels sunk to the lowest levels in five years (Figure 5.2). In the spring after the fire, however, levels reached a maximum of 13 mg/l, the highest value in the time series. This points toward a scenario, where autumn and winter conditions with lower primary production and higher oxygen demand led to low levels being followed by enhanced growth/eutrophication in the following spring. Still, none of these changes were of a great enough magnitude to induce a

change point. This might then explain why the parameter was not well modeled with the existing predictors and CP methodologies.

Another parameter that had bad model performance was COND. Contrary to DO, this parameter had the highest positive rate of all water quality parameters. This, coupled with the bad discriminative abilities of the models suggest high volatility of the parameter. In other words, conductivity typically increases after wildfires, but also probably during times of low flow or through pollution which could be pointwise or as a reaction to land use practices or changes (McDiffett et al. 1989, Boyd 2019). Increases in conductivity seen after wildfires are therefore not only due to the fires but could be also caused by a multitude of other sources. Time series of COND had high interannual variation and seemed to correlate negatively with rainfall (exemplary: Figure 5.3), explaining the bad model performance.

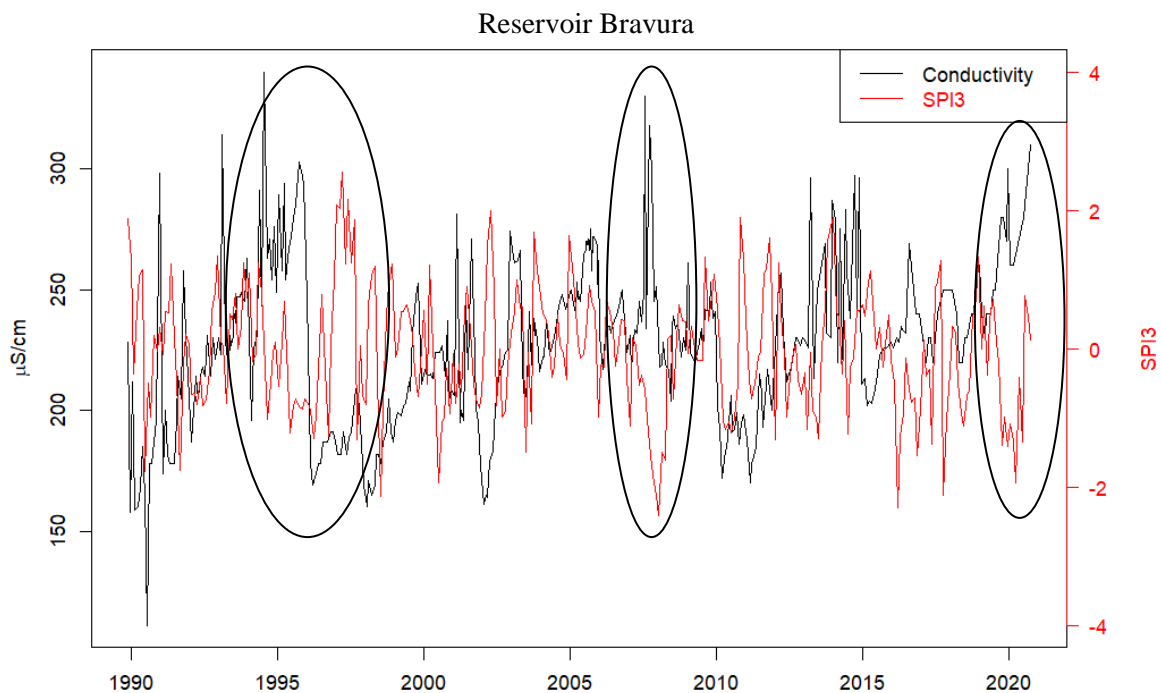


Figure 5.3: Standardized precipitation index with a 3-month accumulation period values from the European Drought Observatory overlaid onto the conductivity timeline of the Bravura reservoir. Encircled are periods, where large increases in SPI correlate visibly with decreases in COND or vice versa. A lag in the SPI3 time series is caused by the 3-month reference period.

In the other water quality constituents, positive rates were much more similar. PH was another parameter with a rather low positive rate and mediocre modeling performance, however, there was a visible trend that only the most significant fires triggered a reaction in pH. This is likely due to the reasons already explained through DO, where reservoir internal processes influence pH levels and the chosen methodology is unable to pick up smaller variabilities. Five increases and three decreases in pH were seen in the CPs of the reservoirs and while largely increases in soil pH are reported after wildfires, fires on already acidic soils with low acid neutralizing capacities can lead to pH decreases in adjacent surface waters (Bayley et al. 1992, Eriksson et al. 2003, Lydersen et al. 2014), although reported in climates of higher altitudes. In the Mediterranean context pH increases are more common.

TSS and the measured nutrients (NO_3 and TP) had similar positive rates, were mildly correlated in their CPs, and achieved the best overall modeling results in terms of differentiating between CP and no CP. So, they are expected to represent post-fire water quality changes best in the current work. These are

also the parameters, together with DOC, that are most often reported in studies about post-fire water quality (Smith et al. 2011). Especially TSS was looked at closer in this work as a possible threatening parameter for water supply. This is due to its correlation with turbidity, which is often a decisive parameter for water supply (Bladon et al. 2014, Martin 2016). 5 mg/l threshold values, proposed by the literature (Langhans et al. 2016), after which water supply is disrupted, were exceeded regularly. As already stated in chapter 4.2.2, TSS values cannot be translated directly to turbidity, and correlation factors vary on a watershed basis, so a margin of error must be included when comparing TSS and turbidity. Still, observed maxima of 8 to 599 mg/l in the 2003-2005 fire-affected watersheds and 18-98 mg/l in 2017 affected watersheds could translate to high turbidity levels. Costs of pre-treatment increase with higher turbidity and higher amounts of dissolved organic carbon (Emelko et al. 2011) and even shutdowns have to be considered if facilities run at high capacity. Turbidity treatment limits in these cases might be around 10-20 NTU (Águas de Portugal, personal communication). Many factors must align for these scenarios to appear, but chances aren't too low. During the meteorological drought of 2004/2005 (García-Herrera et al. 2007) water treatment plants connected to fire-affected watersheds like Bravura or Funcho experienced lower performances than expected, although still maintaining good water quality (Vieira 2009). In this area especially, wildfire seasons coincide with summer tourism, possibly putting pressure on treatment facilities. As water treatment plants can handle different amounts of turbidity, depending on the capacity they are running at, installing higher capacity plants in risk-prone areas can be a viable way to buffer impacts.

5.2 Predictor effects

5.2.1 Main predictors

In terms of predictors, fire size, severity, the IC, post-fire-year reservoir levels, and the pastures BAR showed consistent effects across all parameters, although with different effect sizes. Fire size had an impact on almost all parameters, with larger BAR leading to an increased chance of water quality response. The biggest effects were seen on the nutrients and TSS, where fire size was always a significant predictor. This result is straightforward and in line with earlier research and hypotheses.

In my work, although severity was often chosen as a significant parameter, effect sizes were mostly small, and changes could often be modeled better with fire size instead of severity. Even within severity-based models, effects caused through sediment connectivity were larger overall. The $BAR \geq$ high severity was only chosen for two models, being significant for one of them. In the model where it was chosen as a significant predictor (TSS), the changepoints were modeled better through fire size. These results suggest that high fire severity was not a strong driver of post-fire water quality response in the analyzed fires. Explanations for the deviations between results from the present work and past research could be again found in the study design with a focus on reservoirs or data quality. Effects from severity could be overshadowed by reservoir-related effects such as the reservoir level. For example, the wildfires in 2003-2005 in the south of Portugal had a lower severity than the 2017 wildfires in the center. However, these fires showed the overall greatest effects, likely enhanced due to severe drought and therefore low reservoir levels. The large reservoirs in central Portugal, where the wildfires of 2017 largely happened, were able to buffer the impacts through their large volumes (Basso et al. 2021). On the other hand, differences with other studies could be explained by these studies exploring quantitative changes after fires and not only qualitative changes. Based on the high correlation between $BAR \geq$ low severity and fire size (spearman's $\rho = 0.797$), a more similar effect between at least these two predictors was assumed, so data quality issues described later could also have an influence

The IC was chosen as a predictor in nearly all the models. This was expected since sediment connectivity most closely represents the mechanisms under which post-fire water contamination occurs. However,

as already mentioned the effects could be distorted through outliers. This was evaluated for the nutrients and TSS where the outlier was taken out of the models. New effects were drastically smaller than before and in the case of TSS, the predictor got eliminated from the model completely (Figure 5.4).

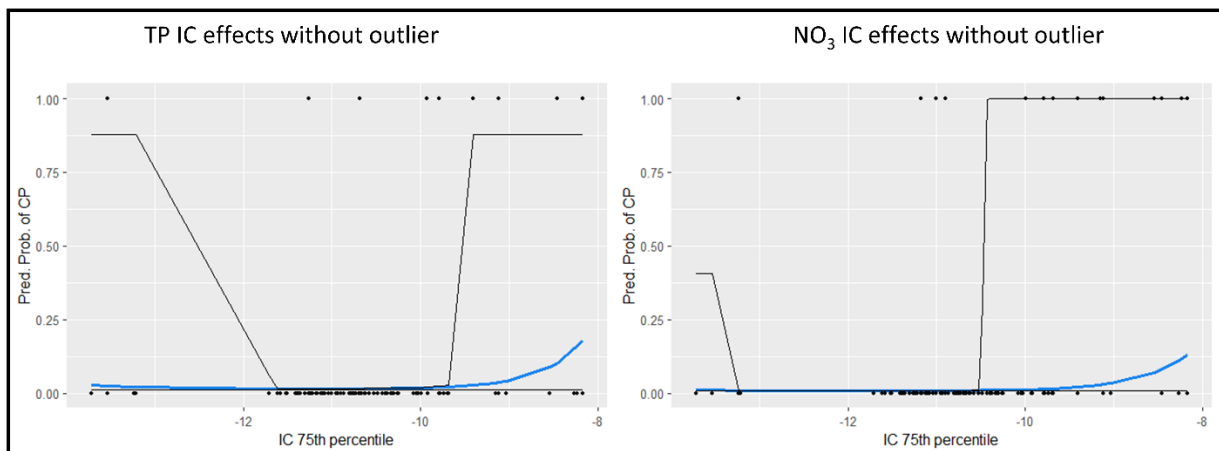


Figure 5.4: Predictor effects of IC on the response of total phosphorous (TP) and nitrate (NO₃), excluding an outlier (Penedo Redondo, 2017). Plots were calculated in the same fashion as the effect plots of chapter 4.3.

Therefore, I don't want to make recommendations about the usefulness of the IC for modeling post-fire changes in water quality. Further studies are needed on what might be the optimal value to represent the IC in such studies, as the 75th percentile value used here might not be ideal to co-represent fire effects and general watershed erosion characteristics.

The reservoir levels represent the only predictor consistent and significant over multiple models that are decoupled from the fire itself. These predictors need to have larger impacts or correlate with big wildfires to be visible in the parameter GAMs. In their occurrence reservoir levels are coupled to large wildfires through drought. Further, low reservoir levels i.e., during droughts can affect reservoir water quality similarly to wildfires (Mosley 2015), making it hard to differentiate between fire and drought impacts in drought-year fires. Nonetheless, this characteristic was identified as an important predictor, especially for NO₃ and TSS impacts. It might be one of the keys to explaining why the 2003-2005 wildfire season resulted in more drastic impacts than the more severe 2017 wildfire season. In this period, countrywide low water levels coincided with large fires leading to impacts on reservoirs, especially in Southern Portugal, but also in the center of Portugal. In these central regions, watersheds that burned in 2017 in similar sizes were less likely to show any impacts. For the parameter models of TSS and NO₃, a post-fire reservoir level threshold value of around 80% water level seems imminent, after which chances for a CP were almost guaranteed. This leaves room for discussion if impacts in these scenarios were mainly caused by drought but since these levels coincided and are expected to coincide with large fires, segregating effects is not necessary. Further, interactions between droughts and wildfire effects are expected, since low water levels not only reduce dilution effects but are also limiting vegetation regrowth, leading to prolonged periods of higher soil erosion (Gouveia et al. 2012).

5.2.2 Further predictors

One predictor, that had consistent effects on the parameter models and therefore should be named was the pasture BAR i.e., the extent of pasture burned, represented as percent of the watershed size. This predictor showed similar effects, although of less magnitude, as fire size or fire severity. However, no clear ecological explanation can be named for that effect. Most likely, it is a confounding effect due to the correlation between fire size, and pasture areas burned. Other characteristics, that might be

interesting to include in future studies are the aridity index and the watershed area to volume ratio. The aridity index showed its largest effects in the TSS model, preferring a CP in subhumid watersheds. While this effect could be due to areas with intermediate aridity being more likely to burn, it might be also caused by the better soils and vegetation cover in humid regions, which could intercept ashes and sediments on their way to streams better than in semi-humid areas. Other reasons, e.g., lower slopes in the humid northwest could be also responsible. The watershed area to volume ratio did show inconsistent effects, likely since interactions were excluded from the models. A test-wise inclusion of a fire size-watershed area to volume ratio interaction revealed some likely small impact on the response of e.g., TP and TSS, favoring impacts in watersheds with a high watershed area to volume ratio (Figure 5.5). So it may be that larger reservoirs can buffer post-fire water quality impacts. A larger sample size is needed

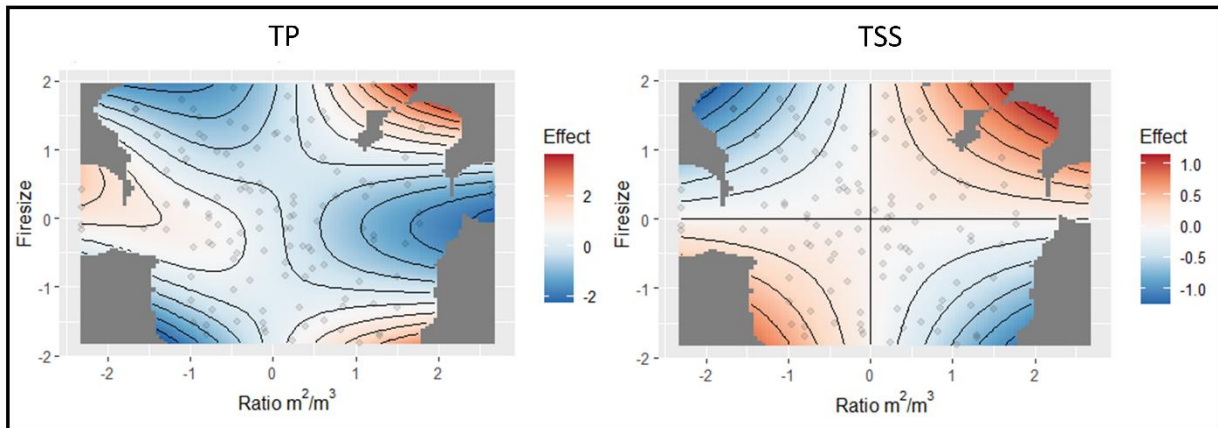


Figure 5.5: Test-wise fire size / watershed-area-to-volume ratio interactions into total phosphorous (TP) and total suspended sediments (TSS) models. Red areas represent a positive impact on effect (so on a changepoint), and dark blue negative impact. Both graphs show positive effects when both fire size and the watershed-area-to-volume ratio were large.

to validate or counter this hypothesis.

5.3 Limitations and possible error sources

This work has three major sources of uncertainty or error, which are namely the parameter time series data themselves, the changepoint analysis, and the modeling process. In the time series data problems regarding detection limits or data gaps were already discussed. Further, the broad sampling frequency could lead to events not being represented during sampling. This was already mitigated by only using reservoirs, where water residency times might be longer, but pollution effects might be diluted. Also, only one station per fire event and reservoir was chosen, so the effects seen in the time series cannot be translated onto the whole reservoir. Although locations were known and consistently near the reservoir outlets, the reservoirs may also be horizontally heterogenic, and therefore measuring locations cannot be compared between reservoirs, sampling depths were not always known and could influence measurements (Thornton et al. 1982).

Another possible source of error was the changepoint analysis. As discussed, during CPA no other possible source of pollution was accounted for. This could introduce several false positives as likely seen in the COND time series. However, most reservoirs used in this analysis are in natural areas with low population density, so human-caused pollution is less likely and constant over time (Boyd 2019). So only broad changes in land use or industrial construction during the fire year may result in false positives. In the case of COND, the errors could be identified through the discriminative performance of the parameter model which was not satisfactory. Since other modeled parameters showed good discriminative performance, it is unlikely that a high number of false positives or true negatives was

introduced by the CPA. Other limitations of the CPA included the violation of some assumptions of the used algorithms. By using a two out of three-detection method (only accepting CPs when at least two algorithms detected one) more data could be included without generating bias from violating assumptions. However, the sensitivity of the CPA likely decreased, so smaller changes may not have been detected.

For the modeling process, uncertainties are in the computation of parameter effects and the error might be enhanced through the imputation of predictor scores. Although multiple imputation is believed to reduce bias compared to complete case analysis (Madley-Dowd et al. 2019), a considerable amount of random errors and variance might be introduced, especially in small datasets (Hardt et al. 2013). In this work, only the predictors of fire severity, IC, and reservoir levels had considerable amounts of missing data. Of these predictors, the random error in reservoir levels introduced through the imputation might be the greatest since the fraction of missing information was the biggest due to low correlations with other complete predictors. In the modeling process itself, uncertainties were represented in the predictor effects. 95% confidence intervals were computed through bootstrapped datasets and shown for each effect. Since positives were sparse for most of the modeled parameters and overall, the models were fitted on rather small amounts of data, the influence of the positives on the predictor effects is large. Uncertainties in the calculated confidence range can therefore be expected to be big. This was observed in the plots of predictor effects, where effect size confidence intervals were ranging from large to non-existent for most predictors. A notable exception is the TSS model, where fire size had a large impact with a relatively small confidence interval. Overall, this highlights that even though the predictors were able to explain events in the given period, they shouldn't be extrapolated or generalized with confidence, except for maybe TSS, which showed smaller confidence intervals and overall good discriminative power.

6 Conclusion

This work was aimed at identifying post-fire water contamination events in Portuguese reservoirs from publicly available time series data. Contaminants of concern and drivers of the contamination events could be identified, loosely following the framework proposed by Nunes et al. (2018) to better understand post-fire water contamination.

All the studied parameters showed impacts of post-fire water contamination in the considered study period and area, although with different frequencies. TP, NO₃, and TSS were identified as the most suitable parameters to identify post-fire water contamination since their reactions could be explained best through the models. They had a changepoint in 9.6-13.6% of times after fires. BOD and COD were promising in the modeling process but limited in their data quality. COND, DO, and pH were not suited to identify post-fire water quality changes in the context of this work. They may still be suitable parameters to measure and interpret if contamination events are already identified or when headwaters and lower-order streams are analyzed.

Areas at risk were identified as areas already prone to burning, but the south of Portugal was disproportionately affected in the study period. This could be attributed to low water levels that coincided with a severe drought for the 2003-2005 wildfire season. The 2017 wildfire season, although bigger and more severe had fewer impacts on the large reservoirs and watersheds that it burned. Smaller reservoirs and watersheds, however, still showed significant impacts. These results point out the importance of considering reservoir levels and potentially other watershed-related characteristics when impacts from wildfires are investigated or modeled. Reservoirs under severe drought stress i.e., with extremely low water levels are especially at risk. With that in mind, fire size was arguably of greatest importance when

determining if a fire led to a reservoir impact, and not all the complex interactions between fire-, watershed-, reservoir-, and climate characteristics could be represented accordingly in the models, which leaves room for further analysis.

This work showed that impact mechanisms of direct parameter reactions in headwaters do not always apply to reservoir impacts. Impact studies, largely conducted in headwaters or lower order streams may not linearly apply downstream, where water supply could be potentially affected. Therefore, the insights from this work can be only partly translated to e.g., impacts in rivers or headwaters, and future studies could address and compare differences in post-fire reactions of lentic and lotic systems along the river continuum. Further research with more inclusive datasets in different temporal or spatial contexts is needed to question or strengthen the general implications gained through the present research. Long-time studies with dense pre- and post-fire sampling intervals could be a key in translating between the abundant case studies and broader dataset-based studies.

It must be said that although a span of over 20 years was assessed, this span only included two major wildfire seasons which differed greatly in their characteristics. This is not necessarily a sample size on which to base widespread conclusions. Nonetheless, it is one of the more extensive datasets analyzed for this purpose. Coupled together with assumptions that drought and other climate change induce extremes may intensify over the next decades (Seneviratne et al. 2021), the problem of post-fire water contamination might most certainly get more likely in the future, at least in Portugal. In my opinion, mixed-use reservoirs, which are used for agricultural irrigation, water supply, and industrial needs, are especially at risk. These reservoirs get used intensively in dry years where water needs are biggest, but also where wildfire risk may be greatest (Pausas and Keeley 2021). Low reservoir levels can then not dilute the impact coming from contaminated sludge streams increasing costs for water supply or even risking outages. To avoid this, integrated water management is needed with a focus on ensuring good drinking water quality. The study of past events, fluctuations in population, and future climate scenarios should determine water treatment capacities in risk-prone regions. If these factors are considered, however, a convincing majority of post-fire water contamination episodes can be absorbed through water treatment, although at higher costs. Studies such as the present one are important to gain an overview of the state of post-fire water quality changes and events that have happened in the past and therefore may happen in future scenarios.

7 Literature Cited

- Abraham, J., K. Dowling, and S. Florentine. 2017*a*. Risk of post-fire metal mobilization into surface water resources: A review. *Science of The Total Environment* **599-600**:1740–1755.
- Abraham, J., K. Dowling, and S. Florentine. 2017*b*. The Unquantified Risk of Post-Fire Metal Concentration in Soil: a Review. *Water, Air, & Soil Pollution* **228**:1–33.
- Abram, N. J., B. J. Henley, A. Sen Gupta, T. J. R. Lippmann, H. Clarke, A. J. Dowdy, J. J. Sharples, R. H. Nolan, T. Zhang, M. J. Wooster, J. B. Wurtzel, K. J. Meissner, A. J. Pitman, A. M. Ukkola, B. P. Murphy, N. J. Tapper, and M. M. Boer. 2021. Connections of climate change and variability to large and extreme forest fires in southeast Australia. *Communications Earth & Environment* **2**:1–17.
- Agência Portuguesa do Ambiente. 2021. Atlas da Água - Albufeiras. https://dados.gov.pt/en/datasets/atlas-da-agua-albufeiras/#_ (September 20, 2022).
- Aminikhangahi, S., and D. J. Cook. 2017. A survey of methods for time series change point detection. *Knowledge and Information Systems* **51**:339–367.
- Ayers, R. S., and D. W. Westcot. 1985. Water quality for agriculture. Food and Agriculture Organization, Rome.
- Bai, J., and P. Perron. 2003. Computation and analysis of multiple structural change models. *Journal of Applied Econometrics* **18**:1–22.
- Basso, M., M. Mateus, T. B. Ramos, and D. C. S. Vieira. 2021. Potential Post-Fire Impacts on a Water Supply Reservoir: An Integrated Watershed-Reservoir Approach. *Frontiers in Environmental Science* **9**.
- Bayley, S. E., D. W. Schindler, B. R. Parker, M. P. Stainton, and K. G. Beaty. 1992. Effects of forest fire and drought on acidity of a base-poor boreal forest stream: similarities between climatic warming and acidic precipitation. *Biogeochemistry* **17**:191–204.
- Beatty, S. M., and J. E. Smith. 2013. Dynamic soil water repellency and infiltration in post-wildfire soils. *Geoderma* **192**:160–172.
- Beck, H. E., N. E. Zimmermann, T. R. McVicar, N. Vergopolan, A. Berg, and E. F. Wood. 2018. Present and future Köppen-Geiger climate classification maps at 1-km resolution. *Scientific data* **5**:180214.
- Beighley, M., and A. C. Hyde. 2018. Portugal wildfire management in a new era assessing fire risks, resources and reforms, Lisboa, Portugal.
- Bijay-Singh, and E. Craswell. 2021. Fertilizers and nitrate pollution of surface and ground water: an increasingly pervasive global problem. *SN Applied Sciences* **3**:1–24.
- Bladon, K. D., M. B. Emelko, U. Silins, and M. Stone. 2014. Wildfire and the future of water supply. *Environmental science & technology* **48**:8936–8943.
- Blake, W. H., P.J. Wallbrink, and I. G. Droppo. 2009. Sediment aggregation and water quality in wildfire-affected river basins. *Marine and Freshwater Research* **60**:653–659.

- Blandford, D. 2019. “Burn Baby Burn” – Controlling the Risk of Wildfires in Greece.
- Borselli, L., P. Cassi, and D. Torri. 2008. Prolegomena to sediment and flow connectivity in the landscape: A GIS and field numerical assessment. *CATENA* **75**:268–277.
- Bowman, D. M. J. S., J. K. Balch, P. Artaxo, W. J. Bond, J. M. Carlson, M. A. Cochrane, C. M. D'Antonio, R. S. Defries, J. C. Doyle, S. P. Harrison, F. H. Johnston, J. E. Keeley, M. A. Krawchuk, C. A. Kull, J. B. Marston, M. A. Moritz, I. C. Prentice, C. I. Roos, A. C. Scott, T. W. Swetnam, G. R. van der Werf, and S. J. Pyne. 2009. Fire in the Earth system. *Science (New York, N.Y.)* **324**:481–484.
- Boyd, C. E. 2019. *Water Quality. An Introduction.* Springer Nature.
- Britton, D. L. 1991. Fire and the chemistry of a South African mountain stream. *Hydrobiologia* **218**:177–192.
- Brune, G. M. 1953. Trap efficiency of reservoirs. *Transactions* **34**:407–418.
- Burke, M. P., T. S. Hogue, A. M. Kinoshita, J. Barco, C. Wessel, and E. D. Stein. 2013. Pre- and post-fire pollutant loads in an urban fringe watershed in Southern California. *Environmental Monitoring and Assessment* **185**:10131–10145.
- Calheiros, T., M. G. Pereira, and J. P. Nunes. 2021. Assessing impacts of future climate change on extreme fire weather and pyro-regions in Iberian Peninsula. *The Science of the total environment* **754**:142233.
- Catry, F. X., F. C. Rego, F. L. Bação, and F. Moreira. 2009. Modeling and mapping wildfire ignition risk in Portugal. *International Journal of Wildland Fire* **18**:921.
- Cerdà, A. 1998. Changes in overland flow and infiltration after a rangeland fire in a Mediterranean scrubland. *Hydrological Processes* **12**:1031–1042.
- Chen, J., and A. K. Gupta. 2012. *Parametric Statistical Change Point Analysis. With Applications to Genetics, Medicine, and Finance.* Birkhäuser Boston, Boston.
- Cohen, J. 2013. *Statistical Power Analysis for the Behavioral Sciences.* Routledge.
- Dahm, C. N., R. I. Candelaria-Ley, C. S. Reale, J. K. Reale, and D. J. van Horn. 2015. Extreme water quality degradation following a catastrophic forest fire. *Freshwater Biology* **60**:2584–2599.
- Darken, P. F., C. E. Zipper, G. I. Holtzman, and E. P. Smith. 2002. Serial correlation in water quality variables: Estimation and implications for trend analysis. *Water Resources Research* **38**:22-1-22-7.
- DeBano, L. F., and J. S. Krammes. 1966. Water repellent Soils and their relation to Wildfire Temperatures. *International Association of Scientific Hydrology. Bulletin* **11**:14–19.
- Direção-Geral do Território. Cartografia de Uso e Ocupação do Solo. <https://snig.dgterritorio.gov.pt/rndg/srv/por/catalog.search#/search?anysnig=cos&fast=index> (August 30, 2022).
- Direção-Geral do Território. 2018. Especificações técnicas da Carta de Uso e Ocupação do Solo de Portugal Continental para 1995, 2007, 2010 e 2015.

- <https://www.dgterritorio.gov.pt/sites/default/files/documentos-publicos/ET-COS-1995-2007-2010-2015.pdf> (September 20, 2022).
- Doerr, S. H., and A. Cerdà. 2005. Fire effects on soil system functioning: new insights and future challenges. *International Journal of Wildland Fire* **14**:339–342.
- Dormann, C. F. 2020. Calibration of probability predictions from machine-learning and statistical models. *Global Ecology and Biogeography* **29**:760–765.
- Dormann, C. F., J. Elith, S. Bacher, C. Buchmann, G. Carl, G. Carré, J. R. García Marquéz, B. Gruber, B. Lafourcade, P. J. Leitão, T. Münkemüller, C. McClean, P. E. Osborne, B. Reineking, B. Schröder, A. K. Skidmore, D. Zurell, and S. Lautenbach. 2013. Collinearity: a review of methods to deal with it and a simulation study evaluating their performance. *Ecography* **36**:27–46.
- Durand, W. M., J. M. DePasse, and A. H. Daniels. 2018. Predictive Modeling for Blood Transfusion After Adult Spinal Deformity Surgery: A Tree-Based Machine Learning Approach. *Spine* **43**:1058.
- Earl, S. R., and D. W. Blinn. 2003. Effects of wildfire ash on water chemistry and biota in South-Western U.S.A. streams. *Freshwater Biology* **48**:1015–1030.
- Eckley, I. A., P. Fearnhead, and R. Killick. 2011. Analysis of changepoint models *in* . *Bayesian Time Series Models*.
- Ekström, J. 2011. The phi-coefficient, the tetrachoric correlation coefficient, and the Pearson-Yule Debate. UCLA: Department of Statistics.
- El Khouli, R. H., K. J. Macura, P. B. Barker, M. R. Habba, M. A. Jacobs, and D. A. Bluemke. 2009. Relationship of temporal resolution to diagnostic performance for dynamic contrast enhanced MRI of the breast. *Journal of magnetic resonance imaging : JMRI* **30**:999–1004.
- Emelko, M. B., U. Silins, K. D. Bladon, and M. Stone. 2011. Implications of land disturbance on drinking water treatability in a changing climate: demonstrating the need for "source water supply and protection" strategies. *Water research* **45**:461–472.
- Emiliano, P. C., M. J.F. Vivanco, and F. S. de Menezes. 2014. Information criteria: How do they behave in different models? *Computational Statistics & Data Analysis* **69**:141–153.
- Emmerton, C. A., C. A. Cooke, S. Hustins, U. Silins, M. B. Emelko, T. Lewis, M. K. Kruk, N. Taube, D. Zhu, B. Jackson, M. Stone, J. G. Kerr, and J. F. Orwin. 2020. Severe western Canadian wildfire affects water quality even at large basin scales. *Water research* **183**:116071.
- Enders, C. K. 2013. Dealing With Missing Data in Developmental Research. *Child Development Perspectives* **7**:27–31.
- Eriksson, H., F. Edberg, and H. Borg. 2003. Effects of forest fire and fire-fighting operations on water chemistry in Tyresta National Park, Stockholm, Sweden. *Journal de Physique IV (Proceedings)* **107**:427–430.
- European Union. 2017. Copernicus Land Monitoring Service - EU-DEM. European Environment Agency. <https://www.eea.europa.eu/data-and-maps/data/copernicus-land-monitoring-service-eu-dem> (August 31, 2022).

- Fernandes, P. M., N. Guiomar, and C. G. Rossa. 2019. Analysing eucalypt expansion in Portugal as a fire-regime modifier. *Science of The Total Environment* **666**:79–88.
- Filkov, A. I., T. Ngo, S. Matthews, S. Telfer, and T. D. Penman. 2020. Impact of Australia's catastrophic 2019/20 bushfire season on communities and environment. Retrospective analysis and current trends. *Journal of Safety Science and Resilience* **1**:44–56.
- Fowler, C. 2003. Human Health Impacts of Forest Fires in the Southern United States: A Literature Review. *Journal of Ecological Anthropology* **7**:39–63.
- García-Herrera, R., E. Hernández, D. Barriopedro, D. Paredes, R. M. Trigo, I. F. Trigo, and M. A. Mendes. 2007. The Outstanding 2004/05 Drought in the Iberian Peninsula: Associated Atmospheric Circulation. *Journal of Hydrometeorology* **8**:483–498.
- Giannaros, T. M., G. Papavasileiou, K. Lagouvardos, V. Kotroni, S. Dafis, A. Karagiannidis, and E. Dragozi. 2022. Meteorological Analysis of the 2021 Extreme Wildfires in Greece: Lessons Learned and Implications for Early Warning of the Potential for Pyroconvection. *Atmosphere* **13**:475.
- Gouveia, C. M., A. Bastos, R. M. Trigo, and C. C. DaCamara. 2012. Drought impacts on vegetation in the pre- and post-fire events over Iberian Peninsula. *Natural Hazards and Earth System Sciences* **12**:3123–3137.
- Granged, A. J.P., A. Jordán, L. M. Zavala, M. Muñoz-Rojas, and J. Mataix-Solera. 2011. Short-term effects of experimental fire for a soil under eucalyptus forest (SE Australia). *Geoderma* **167-168**:125–134.
- Guerrero, C., J. Mataix-Solera, J. Navarro-Pedreño, F. García-Orenes, and I. Gómez. 2001. Different Patterns of Aggregate Stability in Burned and Restored Soils. *Arid Land Research and Management* **15**:163–171.
2011. Guidelines for drinking-water quality. World Health Organization, Geneva.
- Gurarie, E. 2014. bcpa: Behavioral change point analysis of animal movement.
- Gurarie, E., R. D. Andrews, and K. L. Laidre. 2009. A novel method for identifying behavioural changes in animal movement data. *Ecology letters* **12**:395–408.
- Hallema, D. W., A. M. Kinoshita, D. A. Martin, F.-N. Robinne, and P. F. Moore. 2019. Fire, forests and city water supplies. *Unasylva* **251**:58–66.
- Hallema, D. W., G. Sun, P. V. Caldwell, S. P. Norman, E. C. Cohen, Y. Liu, K. D. Bladon, and S. G. McNulty. 2018. Burned forests impact water supplies. *Nature communications* **9**:1307.
- Hardt, J., M. Herke, T. Brian, and W. Laubach. 2013. Multiple Imputation of Missing Data: A Simulation Study on a Binary Response. *Open Journal of Statistics* **03**:370–378.
- Harrell Jr., F. E. 2022. Hmisc: Harrell Miscellaneous.
- Haynes, K., I. A. Eckley, and P. Fearnhead. 2017a. Computationally Efficient Changepoint Detection for a Range of Penalties. *Journal of Computational and Graphical Statistics* **26**:134–143.
- Haynes, K., P. Fearnhead, and I. A. Eckley. 2017b. A computationally efficient nonparametric approach for changepoint detection. *Statistics and computing* **27**:1293–1305.

- Haynes, K., R. Killick, P. Fearnhard, and I. Eckley. 2016. *changept*. np: Methods for nonparametric changepoint detection.
- Higuera, P. E., and J. T. Abatzoglou. 2021. Record-setting climate enabled the extraordinary 2020 fire season in the western United States. *Global change biology* **27**:1–2.
- Holliday, C. P., T. C. Rasmussen, and W. P. Miller. 2001. Establishing the Relationship between Turbidity and Total Suspended Sediment Concentration *in* K. J. Hatcher, editor. Proceedings of the 2003 Georgia Water Resources Conference. April 23-24, 2003, Athens, Georgia. Institute of Ecology, University of Georgia, Athens, Ga., U.S.A.
- Hulsmann, A. D. 2011. The quality of drinking water in the European Union 2005-2007. Synthesis report on the quality of drinking water in the Member States of the European Union in the period 2005-2007 Directive 98/83/EC.
- Instituto da Conservação da Natureza e das Florestas. 2004. Índice de Aridez 2000/2010. <https://snig.dgterritorio.gov.pt/rndg/srv/api/records/bc8411c2-3321-495b-a080-f5ff30d64cad/formatters/snig-view> (September 20, 2022).
- Instituto da Conservação da Natureza e das Florestas. 2022. Territórios arditos (Área ardida entre 1975 e 2021). Instituto da Conservação da Natureza e das Florestas. https://geocatalogo.icnf.pt/catalogo_tema5.html (September 20, 2022).
- IPMA. Clima Normais. <https://www.ipma.pt/pt/oclima/normais.clima/?print=true> (August 23, 2022).
- Jesus, M. R. de. 2001. Groundwater Protection for Public Water-Supply in Portugal, Lisboa, Portugal.
- Johnson, D., J. D. Murphy, R. F. Walker, D. W. Glass, and W. W. Miller. 2007. Wildfire effects on forest carbon and nutrient budgets. *Ecological Engineering* **31**:183–192.
- Jolly, W. M., M. A. Cochrane, P. H. Freeborn, Z. A. Holden, T. J. Brown, G. J. Williamson, and D. M. J. S. Bowman. 2015. Climate-induced variations in global wildfire danger from 1979 to 2013. *Nature Communications* **6**:1–11.
- Jones, M. W., A. J. P. Smith, R. Betts, J. G. Canadell, I. C. Prentice, and C. Le Quéré. 2020. Climate Change Increases the Risk of Wildfires: January 2020. *ScienceBrief*.
- Keeley, J. E., W. J. Bond, R. A. Bradstock, J. G. Pausas, and P. W. Rundel. 2011. *Fire in Mediterranean Ecosystems*. Ecology, Evolution and Management. Cambridge University Press.
- Key, C. H., and N. C. Benson. 2006. Landscape Assessment (LA). In: Lutes, Duncan C.; Keane, Robert E.; Caratti, John F.; Key, Carl H.; Benson, Nathan C.; Sutherland, Steve; Gangi, Larry J. 2006. FIREMON: Fire effects monitoring and inventory system. Gen. Tech. Rep. RMRS-GTR-164-CD. Fort Collins, CO: U.S. Department of Agriculture, Forest Service, Rocky Mountain Research Station. p. LA-1-55 **164**.
- Khatri, N., and S. Tyagi. 2015. Influences of natural and anthropogenic factors on surface and groundwater quality in rural and urban areas. *Frontiers in Life Science* **8**:23–39.
- Killick, R., C. Beaulieu, S. Taylor, and H. Hullait. 2021. *EnvCpt: Detection of Structural Changes in Climate and Environment Time Series*.

- Killick, R., and I. Eckley. 2014. changepoint: an R package for changepoint analysis. *Journal of Statistical Software* **58**:1–19.
- Killick, R., P. Fearnhead, and I. A. Eckley. 2012. Optimal Detection of Changepoints With a Linear Computational Cost. *Journal of the American Statistical Association* **107**:1590–1598.
- Kleiber, C., K. Hornik, F. Leisch, and A. Zeileis. 2002. strucchange: An R Package for Testing for Structural Change in Linear Regression Models. American Statistical Association.
- Lane, P. N.J., G. J. Sheridan, P. J. Noske, and C. B. Sherwin. 2008. Phosphorus and nitrogen exports from SE Australian forests following wildfire. *Journal of Hydrology* **361**:186–198.
- Langhans, C., H. G. Smith, D. M.O. Chong, P. Nyman, P. N.J. Lane, and G. J. Sheridan. 2016. A model for assessing water quality risk in catchments prone to wildfire. *Journal of Hydrology* **534**:407–426.
- Leon, A. C., and M. Heo. 2009. Sample Sizes Required to Detect Interactions between Two Binary Fixed-Effects in a Mixed-Effects Linear Regression Model. *Computational Statistics & Data Analysis* **53**:603–608.
- Lindenmayer, D. B., G. E. Likens, and J. F. Franklin. 2010. Rapid responses to facilitate ecological discoveries from major disturbances. *Frontiers in Ecology and the Environment* **8**:527–532.
- Lizundia-Loiola, J., G. Otón, R. Ramo, and E. Chuvieco. 2020. A spatio-temporal active-fire clustering approach for global burned area mapping at 250 m from MODIS data. *Remote Sensing of Environment* **236**:111493.
- Lotspeich, F. B., E. W. Mueller, and P. J. Frey. 1970. Effects of Large Scale Forest Fires on Water Quality in Interior Alaska. U.S. Federal Water Pollution Control Administration, Alaska Water Laboratory.
- Lydersen, E., R. Høgberget, C. E. Moreno, Ø. A. Garmo, and P. C. Hagen. 2014. The effects of wildfire on the water chemistry of dilute, acidic lakes in southern Norway. *Biogeochemistry* **119**:109–124.
- Madley-Dowd, P., R. Hughes, K. Tilling, and J. Heron. 2019. The proportion of missing data should not be used to guide decisions on multiple imputation. *Journal of clinical epidemiology* **110**:63–73.
- Manel, S., J.-M. Dias, and S. J. Ormerod. 1999. Comparing discriminant analysis, neural networks and logistic regression for predicting species distributions: a case study with a Himalayan river bird. *Ecological Modelling* **120**:337–347.
- Mansilha, C., A. Carvalho, P. Guimarães, and J. Espinha Marques. 2014. Water Quality Concerns Due to Forest Fires: Polycyclic Aromatic Hydrocarbons (PAH) Contamination of Groundwater From Mountain Areas. *Journal of Toxicology and Environmental Health, Part A* **77**:806–815.
- Marcot, B. G., and A. M. Hanea. 2021. What is an optimal value of k in k-fold cross-validation in discrete Bayesian network analysis? *Computational Statistics* **36**:2009–2031.
- Marques, S., J. G. Borges, J. Garcia-Gonzalo, F. Moreira, J. M. B. Carreiras, M. M. Oliveira, A. Cantarinha, B. Botequim, and J. M. C. Pereira. 2011. Characterization of wildfires in Portugal. *European Journal of Forest Research* **130**:775–784.

- Marra, G., and S. N. Wood. 2011. Practical variable selection for generalized additive models. *Computational Statistics & Data Analysis* **55**:2372–2387.
- Martin, D. A. 2016. At the nexus of fire, water and society. *Philosophical Transactions of the Royal Society B: Biological Sciences* **371**:20150172.
- Mataix-Solera, J., and S.H. Doerr. 2004. Hydrophobicity and aggregate stability in calcareous topsoils from fire-affected pine forests in southeastern Spain. *Geoderma* **118**:77–88.
- Mayor, A. G., S. Bautista, J. Llovet, and J. Bellot. 2007. Post-fire hydrological and erosional responses of a Mediterranean landscape: Seven years of catchment-scale dynamics. *CATENA* **71**:68–75.
- McDiffett, W. F., A. W. Beidler, T. F. Dominick, and K. D. McCrea. 1989. Nutrient concentration-stream discharge relationships during storm events in a first-order stream. *Hydrobiologia* **179**:97–102.
- McGilchrist, C. A., and K. D. Woodyer. 1975. Note on a Distribution-Free CUSUM Technique. *Technometrics* **17**:321–325.
- McKee, T. B., N. J. Doesken, and J. Kleist. 1993. The relationship of drought frequency and duration to time scales. *Proceedings of the 8th Conference on Applied Climatology* **17**:179–183.
- Meurant, G. 2012. *The Ecology of Natural Disturbance and Patch Dynamics*. Academic Press.
- Millennium Ecosystem Assessment. 2005. *Ecosystems and human well-being: Synthesis*. Island Press, Washington D.C.
- Miller, J. 2010. Species Distribution Modeling. *Geography Compass* **4**:490–509.
- Moghli, A., V. M. Santana, M. J. Baeza, E. Pastor, and S. Soliveres. 2021. Fire Recurrence and Time Since Last Fire Interact to Determine the Supply of Multiple Ecosystem Services by Mediterranean Forests. *Ecosystems*:1–13.
- Mosley, L. M. 2015. Drought impacts on the water quality of freshwater systems; review and integration. *Earth-Science Reviews* **140**:203–214.
- NASA Earth Observatory. 2021. Fires Raged in the Amazon Again in 2020. NASA. <https://earthobservatory.nasa.gov/images/147946/fires-raged-in-the-amazon-again-in-2020> (September 14, 2022).
- Neary, D. G., K. C. Ryan, and L. F. DeBano. 2005. *Wildland fire in ecosystems: effects of fire on soils and water*. U.S. Department of Agriculture, Forest Service, Rocky Mountain Research Station, Ogden UT.
- Nelder, J. A., and R. W. M. Wedderburn. 1972. Generalized Linear Models. *Journal of the Royal Statistical Society. Series A (General)* **135**:370.
- Neris, J., C. Santin, R. Lew, P. R. Robichaud, W. J. Elliot, S. A. Lewis, G. Sheridan, A.-M. Rohlfs, Q. Ollivier, L. Oliveira, and S. H. Doerr. 2021. Designing tools to predict and mitigate impacts on water quality following the Australian 2019/2020 wildfires: Insights from Sydney's largest water supply catchment. *Integrated environmental assessment and management* **17**:1151–1161.

- Nunes, A. N., L. Lourenço, and A. C. Meira. 2016. Exploring spatial patterns and drivers of forest fires in Portugal (1980–2014). *Science of The Total Environment* **573**:1190–1202.
- Nunes, J. P., S. H. Doerr, G. Sheridan, J. Neris, C. Santín, M. B. Emelko, U. Silins, P. R. Robichaud, W. J. Elliot, and J. Keizer. 2018. Assessing water contamination risk from vegetation fires: Challenges, opportunities and a framework for progress. *Hydrological Processes* **32**:687–694.
- Nunes, L., J. P. Monteiro, M. C. Cunha, J. Vieira, H. Lucas, and L. Ribeiro. 2006. The Water Crisis In Southern Portugal: How Did We Get There And How Should We Solve It. *WIT Transactions on Ecology and the Environment* **99**.
- Nunes, M. C.S., M. J. Vasconcelos, J. M.C. Pereira, N. Dasgupta, R. J. Alldredge, and F. C. Rego. 2005. Land Cover Type and Fire in Portugal: Do Fires Burn Land Cover Selectively? *Landscape Ecology* **20**:661–673.
- Oksanen, J., F. G. Blanchet, M. Friendly, R. Kindt, P. Legendre, D. McGlenn, P. R. Minchin, R. B. O'Hara, G. L. Simpson, P. Solymos, M. Henry H., E. Szoecs, and H. Wagner. 2020. *vegan*: Community Ecology Package.
- Parente, J., A. Girona-García, A. R. Lopes, J. J. Keizer, and D. C. S. Vieira. 2022a. Prediction, validation, and uncertainties of a nation-wide post-fire soil erosion risk assessment in Portugal. *Scientific Reports* **12**:1–13.
- Parente, J., J. P. Nunes, J. Baartman, and D. Föllmi. 2022b. Testing simple approaches to map sediment mobilization hotspots after wildfires. Manuscript submitted for publication.
- Pausas, J. G., and J. E. Keeley. 2021. Wildfires and global change. *Frontiers in Ecology and the Environment* **19**:387–395.
- Pearce, J., and S. Ferrier. 2000. An evaluation of alternative algorithms for fitting species distribution models using logistic regression. *Ecological Modelling* **128**:127–147.
- Pereira, P., I. Bogunovic, W. Zhao, and D. Barcelo. 2021. Short-term effect of wildfires and prescribed fires on ecosystem services. *Current Opinion in Environmental Science & Health* **22**:100266.
- Peterson, R. A. 2021. Finding Optimal Normalizing Transformations via bestNormalize. *The R Journal* **13**:310–329.
- Petropoulos, G. P., H. M. Griffiths, and D. P. Kalivas. 2014. Quantifying spatial and temporal vegetation recovery dynamics following a wildfire event in a Mediterranean landscape using EO data and GIS. *Applied Geography* **50**:120–131.
- Prosser, I. P., and L. Williams. 1998. The effect of wildfire on runoff and erosion in native Eucalyptus forest. *Hydrological Processes* **12**:251–265.
- Pyra, N., and S. N. Wood. 2015. Shape constrained additive models. *Statistics and Computing* **25**:543–559.
- QGIS Development Team. 2021. QGIS Geographic Information System. QGIS Association.

- R Core Team. 2021. R: A language and environment for statistical. R Foundation for Statistical Computing, Vienna, Austria.
- Reale, J. K., D. J. van Horn, K. E. Condon, and C. N. Dahm. 2015. The effects of catastrophic wildfire on water quality along a river continuum. *Freshwater Science* **34**:1426–1442.
- Rhoades, C. C., J. P. Nunes, U. Silins, and S. H. Doerr. 2019. The influence of wildfire on water quality and watershed processes: new insights and remaining challenges. *International Journal of Wildland Fire* **28**:721–725.
- Robinne, F.-N., K. D. Bladon, C. Miller, M.-A. Parisien, J. Mathieu, and M. D. Flannigan. 2018. A spatial evaluation of global wildfire-water risks to human and natural systems. *The Science of the total environment* **610-611**:1193–1206.
- Robinne, F.-N., D. W. Hallema, K. D. Bladon, M. D. Flannigan, G. Boisramé, C. M. Bréthaut, S. H. Doerr, G. Di Baldassarre, L. A. Gallagher, A. K. Hohner, S. J. Khan, A. M. Kinoshita, R. Mordecai, J. P. Nunes, P. Nyman, C. Santín, G. Sheridan, C. R. Stoof, M. P. Thompson, J. M. Waddington, and Y. Wei. 2021. Scientists' warning on extreme wildfire risks to water supply. *Hydrological Processes* **35**:e14086.
- Rügner, H., M. Schwientek, B. Beckingham, B. Kuch, and P. Grathwohl. 2013. Turbidity as a proxy for total suspended solids (TSS) and particle facilitated pollutant transport in catchments. *Environmental Earth Sciences* **69**:373–380.
- Russo, A., C. M. Gouveia, P. Páscoa, C. C. DaCamara, P. M. Sousa, and R. M. Trigo. 2017. Assessing the role of drought events on wildfires in the Iberian Peninsula. *Agricultural and Forest Meteorology* **237-238**:50–59.
- Rust, A. J., T. S. Hogue, S. Saxe, and J. McCray. 2018. Post-fire water-quality response in the western United States. *International Journal of Wildland Fire* **27**:203.
- Rust, A. J., S. Saxe, J. McCray, C. C. Rhoades, and T. S. Hogue. 2019. Evaluating the factors responsible for post-fire water quality response in forests of the western USA. *International Journal of Wildland Fire* **28**:769.
- Ryan, K. C., E. E. Knapp, and J. M. Varner. 2013. Prescribed fire in North American forests and woodlands: history, current practice, and challenges. *Frontiers in Ecology and the Environment* **11**.
- Sahin, E. K. 2020. Assessing the predictive capability of ensemble tree methods for landslide susceptibility mapping using XGBoost, gradient boosting machine, and random forest. *SN Applied Sciences* **2**:1–17.
- San-Miguel-Ayanz, J., T. Durrant, R. Boca, P. Maianti, G. Libertà, T. Artés Vivancos, D. Oom, A. Branco, D. Tomàs Rigo, D. Ferrari, H. Pfeiffer, R. Grecchi, D. Nuijten, M. Onida, and P. Löffler. 2021. *Forest Fires in Europe, Middle East and North Africa 2020*. Publications Office of the European Union, Luxembourg.
- San-Miguel-Ayanz, J., J. M. Moreno, and A. Camia. 2013. Analysis of large fires in European Mediterranean landscapes: Lessons learned and perspectives. *Forest Ecology and Management* **294**:11–22.

- Santana, V. M., M. Jaime Baeza, R. H. Marrs, and V. Ramón Vallejo. 2010. Old-field secondary succession in SE Spain: can fire divert it? *Plant Ecology* **211**:337–349.
- Saxe, S., T. S. Hogue, and L. Hay. 2018. Characterization and evaluation of controls on post-fire streamflow response across western US watersheds. *Hydrology and Earth System Sciences* **22**:1221–1237.
- Schindler, D. W. 2012. The dilemma of controlling cultural eutrophication of lakes. *Proceedings. Biological sciences* **279**:4322–4333.
- Schindler, D. W., R. W. Newbury, K. G. Beaty, J. Prokopowich, T. Ruszczynski, and J. A. Dalton. 1980. Effects of a Windstorm and Forest Fire on Chemical Losses from Forested Watersheds and on the Quality of Receiving Streams. *Canadian Journal of Fisheries and Aquatic Sciences* **37**:328–334.
- Seneviratne, S. I., X. Zhang, M. Adnan, W. Badi, C. Dereczynski, A. Di Luca, S. Ghosh, I. Iskandar, J. Kossin, S. Lewis, F. Otto, I. Pinto, M. Satoh, S.M. Vicente-Serrano, M. Wehner, and B. Zhou, editors. 2021. *Weather and Climate Extreme Events in a Changing Climate*. Cambridge University Press, Cambridge, United Kingdom and New York, NY, USA.
- Shakesby, R. A. 2011. Post-wildfire soil erosion in the Mediterranean: Review and future research directions. *Earth-Science Reviews* **105**:71–100.
- Shakesby, R. A., and S. H. Doerr. 2006. Wildfire as a hydrological and geomorphological agent. *Earth-Science Reviews* **74**:269–307.
- Shapiro, S. S., and M. B. Wilk. 1965. An Analysis of Variance Test for Normality (Complete Samples). *Biometrika* **52**:591.
- Sherson, L. R., D. J. van Horn, J. D. Gomez-Velez, L. J. Crossey, and C. N. Dahm. 2015. Nutrient dynamics in an alpine headwater stream: use of continuous water quality sensors to examine responses to wildfire and precipitation events. *Hydrological Processes* **29**:3193–3207.
- Silva, J. M. N., M. V. Moreno, Y. Le Page, D. Oom, I. Bistinas, and J. M. C. Pereira. 2019. Spatiotemporal trends of area burnt in the Iberian Peninsula, 1975–2013. *Regional Environmental Change* **19**:515–527.
- Smith, H. G., G. J. Sheridan, P. N.J. Lane, P. Nyman, and S. Haydon. 2011. Wildfire effects on water quality in forest catchments: A review with implications for water supply. *Journal of Hydrology* **396**:170–192.
- Son, J.-H., S. Kim, and K. H. Carlson. 2015. Effects of Wildfire on River Water Quality and Riverbed Sediment Phosphorus. *Water, Air, & Soil Pollution* **226**:1–13.
- Soto, B., R. Basanta, E. Benito, R. Pérez, and F. Díaz-Fierros. 1991. Runoff and erosion from burnt soils in Northwest Spain. Pages 91–98 *in* M. Sala and J. L. Rubio, editors. *Soil erosion as a consequence of forest fires*. Geofoma Ediciones, Logroño.
- Stagge, J. H., I. Kohn, L. M. Tallaksen, and K. Stahl. 2015. Modeling drought impact occurrence based on meteorological drought indices in Europe. *Journal of Hydrology* **530**:37–50.

- Stanton, J. M. 2001. Galton, Pearson, and the Peas: A Brief History of Linear Regression for Statistics Instructors. *Journal of Statistics Education* **9**:null-null.
- Tan, G., P. Chen, J. Deng, Q. Xu, R. Tang, Z. Feng, and R. Yi. 2019. Review and improvement of conventional models for reservoir sediment trapping efficiency. *Heliyon* **5**:e02458.
- Taylan, P., G.-W. Weber, and A. Beck. 2007. New approaches to regression by generalized additive models and continuous optimization for modern applications in finance, science and technology. *Optimization* **56**:675–698.
- Thornton, K. W., R. H. Kennedy, A. D. Magoun, and G. E. Saul. 1982. Reservoir Water Quality Sampling Design. *Journal of the American Water Resources Association* **18**:471–480.
- Tiedemann, A. R. 1979. Effects of Fire on Water. A State-of-knowledge Review. Department of Agriculture, Forest Service.
- Tiedemann, A. R., J. D. Helvey, and T. D. Anderson. 1978. Stream Chemistry and Watershed Nutrient Economy Following Wildfire and Fertilization in Eastern Washington. *Journal of Environmental Quality* **7**:580–588.
- Tinker, P.B., J. S.I. Ingram, and S. Struwe. 1996. Effects of slash-and-burn agriculture and deforestation on climate change. *Agriculture, Ecosystems & Environment* **58**:13–22.
- Trigo, R. M., P. M. Sousa, M. G. Pereira, D. Rasilla, and C. M. Gouveia. 2016. Modelling wildfire activity in Iberia with different atmospheric circulation weather types. *International Journal of Climatology* **36**:2761–2778.
- Truong, C., L. Oudre, and N. Vayatis. 2020. Selective review of offline change point detection methods. *Signal Processing* **167**:107299.
- Turco, M., J. Bedia, F. Di Liberto, P. Fiorucci, J. von Hardenberg, N. Koutsias, M.-C. Llasat, F. Xystrakis, and A. Provenzale. 2016. Decreasing Fires in Mediterranean Europe. *PloS one* **11**:e0150663.
- Turco, M., S. Jerez, S. Augusto, P. Tarín-Carrasco, N. Ratola, P. Jiménez-Guerrero, and R. M. Trigo. 2019. Climate drivers of the 2017 devastating fires in Portugal. *Scientific Reports* **9**:1–8.
- United States Environmental Protection Agency. 1996. Practical Methods for Data Analysis. Guidance for Data Quality Assessment. EPA QA/G-9.
- USGS. 2020. How Wildfires Threaten U.S. Water Supplies. United States Geological Survey. <https://labs.waterdata.usgs.gov/visualizations/fire-hydro/index.html#/> (September 16, 2022).
- van Buuren, S., and K. Groothuis-Oudshoorn. 2011. mice: Multivariate Imputation by Chained Equations in R. *Journal of Statistical Software* **45**:1–67.
- Varela, M. E., E. Benito, and E. de Blas. 2005. Impact of wildfires on surface water repellency in soils of northwest Spain. *Hydrological Processes* **19**:3649–3657.
- Vieira, P. A. R. 2009. Avaliação de desempenho de estações de tratamento de água para consumo humano.

- Williams, A. P., J. T. Abatzoglou, A. Gershunov, J. Guzman-Morales, D. A. Bishop, J. K. Balch, and D. P. Lettenmaier. 2019. Observed Impacts of Anthropogenic Climate Change on Wildfire in California. *Earth's Future* **7**:892–910.
- Wood, S. N. 2006. *Generalized Additive Models*. Chapman and Hall/CRC.
- Wood, S. N. 2011. Fast stable restricted maximum likelihood and marginal likelihood estimation of semiparametric generalized linear models. *Journal of the Royal Statistical Society (B)* **73**:3–36.
- Woods, S. W., and V. N. Balfour. 2010. The effects of soil texture and ash thickness on the post-fire hydrological response from ash-covered soils. *Journal of Hydrology* **393**:274–286.
- Wu, C., S. Venevsky, S. Sitch, L. M. Mercado, C. Huntingford, and A. C. Staver. 2021. Historical and future global burned area with changing climate and human demography. *One Earth* **4**:517–530.
- Xu, W., Y. Liu, S. Veraverbeke, W. Wu, Y. Dong, and W. Lu. 2021. Active Fire Dynamics in the Amazon: New Perspectives From High-Resolution Satellite Observations. *Geophysical Research Letters* **48**.
- Yang, J., H. Tian, B. Tao, W. Ren, J. Kush, Y. Liu, and Y. Wang. 2014. Spatial and temporal patterns of global burned area in response to anthropogenic and environmental factors: Reconstructing global fire history for the 20th and early 21st centuries. *Journal of Geophysical Research: Biogeosciences* **119**:249–263.
- Young, M., and M. H. Carr. 2015. Application of species distribution models to explain and predict the distribution, abundance and assemblage structure of nearshore temperate reef fishes. *Diversity and Distributions* **21**:1428–1440.
- Zeileis, A., F. Leisch, K. Hornik, and C. Kleiber. 2002. strucchange: An R Package for Testing for Structural Change in Linear Regression Models. *Journal of Statistical Software* **7**:1–38.
- Zipkin, E. F., E. H. Campbell Grant, and W. F. Fagan. 2012. Evaluating the predictive abilities of community occupancy models using AUC while accounting for imperfect detection. *Ecological Applications* **22**:1962–1972.
- Zou, C., G. Yin, L. Feng, and Z. Wang. 2014. Nonparametric maximum likelihood approach to multiple change-point problems. *The Annals of Statistics* **42**.
- Zurell, D., F. Jeltsch, C. F. Dormann, and B. Schröder. 2009. Static species distribution models in dynamically changing systems: how good can predictions really be? *Ecography* **32**:733–744.

Appendix

A.1 Study area

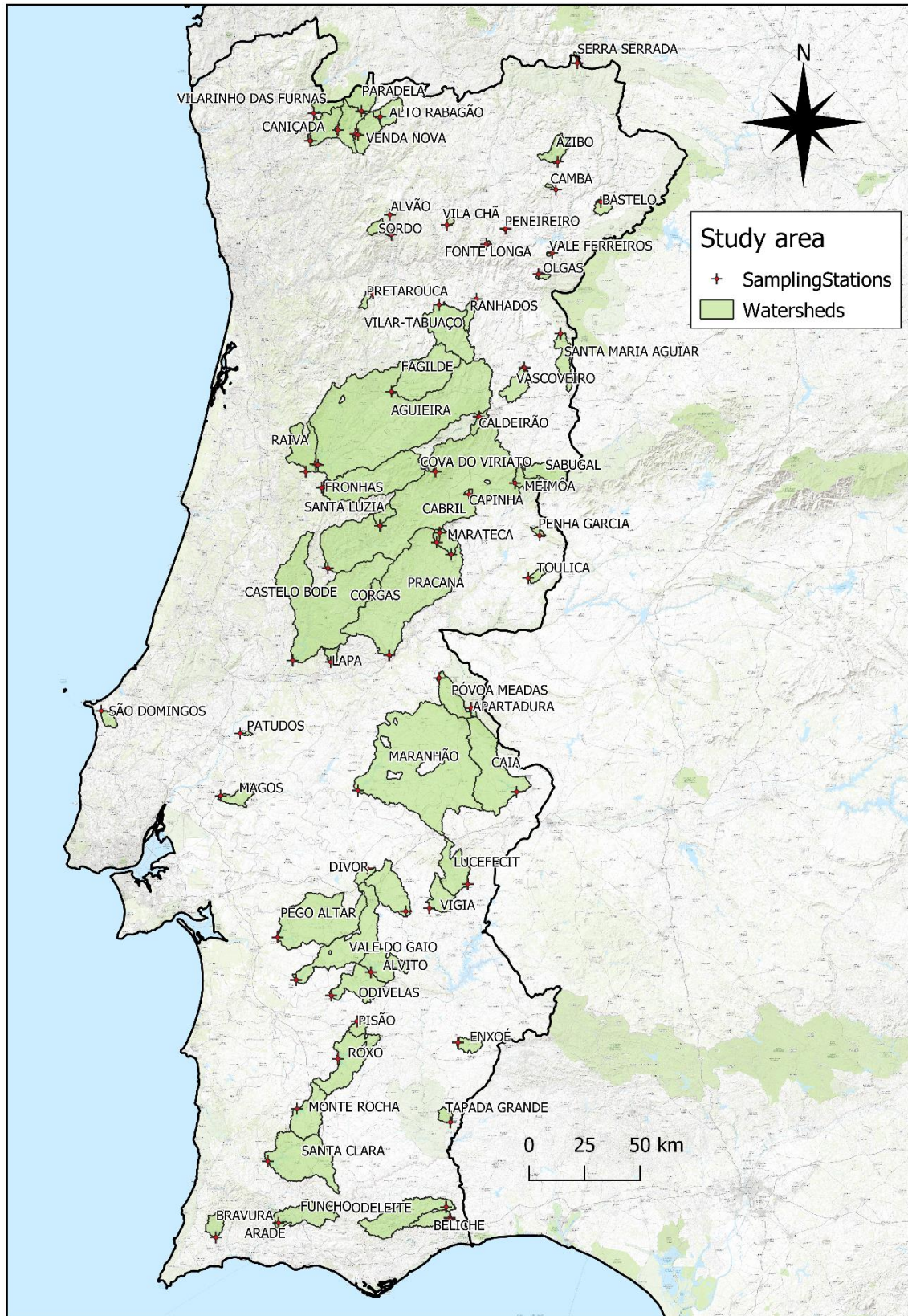


Figure AF.1: Detailed map of the analyzed reservoirs and the used sampling stations of the SNIRH network. The names refer to the reservoir names used in SNIRH.

A.2 Calculation of watersheds

The watersheds were calculated in QGIS (QGIS Development Team 2021) from the European Union digital elevation model (EU-DEM), which is available in a 25x25 m grid cell size (European Union 2017). The resulting watersheds were compared to watersheds generated for the Atlas da Água (Agência Portuguesa do Ambiente 2021) and further compared to watersheds generated for the new EU Water Framework Directive (Directive 2000/60/EC), to assess the quality of the computations. When a watershed of a reservoir contained other notable reservoirs, the watershed of that reservoir was either cut from or remained in the original watershed based on the trapping efficiency (TE) of the newfound reservoir. This was done to not inflate watershed size and include fires that would not affect the downstream watershed when e.g., sediments wouldn't pass a dam, or the reservoir could act as a nutrient sink. TE was estimated after methods explained and evaluated in Brune 1953, Tan et al. 2019). Capacity-inflow ratios were preferred over capacity-watershed ratios if data was available. Where little to no data was available capacity was estimated through satellite imagery. A sub-watershed was cut from the original watershed when the TE was estimated at above 80%.

A.3 Origin and calculation of regression analysis predictor variables

Fire size: Yearly fire size was already fully available as polygons of BA in yearly shapefile format from the Portuguese Institute of Forests and Nature Conservation (Instituto da Conservação da Natureza e das Florestas 2022). All BAs of a year were clipped to the reservoir watershed, added up, and divided by the total watershed area to obtain the BAR.

Fire severity: Fire severity was obtained from other FRISCO projects. For this Landsat and MODIS satellite imagery was taken before and after the fires and the Δ Normalized-Burned-Ratio was computed. Thresholds from Key and Benson (2006) were used to determine areas with low, medium, and high fire severity.

Land use: The land use data was taken from Cartografia de Uso e Ocupação do Solo (COS) map versions 1995, 2007, 2010, and 2015 (Direção-Geral do Território)(Direção-Geral do Território 2018) and clipped to the reservoir watersheds. The land use which was close to the fire year without laying in or exceeding the fire year was chosen to represent the land use data for a given fire year. Only the categories of Eucalypts, other broadleaf forests, coniferous forests, shrub land, and pastures were considered as they can be best linked with fire scenarios and represent the largest part of yearly BA. The land use types were identified according to the land use classes of COS 1995 as this version gives the least detailed nomenclature of land use classes. The above-mentioned land use types were converted to the BAR of the given land use type, to disconnect them as much as possible from fire size.

Sediment connectivity: For sediment connectivity, the IC, proposed by Borselli et al. (2008) was used. The IC was calculated in map form by FRISCO members from the above-taken fire severity maps and COS Land cover and topographic maps. Information on the calculation of the IC can be found in the above-mentioned paper. The fire severity in this case determines the C-factor of the IC. COS Land use maps were taken as the closest available version before the fire year. After the map calculation, the 75th percentile value of the IC map for a given watershed was extracted to represent sediment connectivity in the logistic regression. The IC identifies sediment mobilization after wildfires in areas of erosion rates above the 75th percentile (Parente et al. 2022b). However other values, such as e.g., the mean, median or 95th percentile could be also taken to represent the watershed since the ideal value to represent IC is not explored nor in the scope of this work.

Watershed-area-to-volume ratio: Reservoir volumes for the reservoir-volume-to-watershed-size-ratio were also mostly obtained from SNIRH (<https://snirh.apambiente.pt/>), with missing reservoirs being

added through direct information from reservoir operators or media articles. Watershed areas were taken from the calculated watersheds.

Aridity index: The aridity index was taken as a shapefile with polygons of the different aridity levels from the ICNF (Instituto da Conservação da Natureza e das Florestas 2004). The map was clipped to the watersheds and the mean value of aridity was taken from every watershed (with values ranging from 1-5). The 2000 to 2010 index was used as it was least biased for the data while a newer index with a longer reference period was unavailable.

Standardized Precipitation Index (SPI): The SPI with a 12-month reference period was obtained from the Global Drought Observatory (McKee et al. 1993). SPI12 values of October 1st were chosen for the pre-fire, fire, post-fire, and 2-year-post-fire years, to represent the hydrological years. SPI12 in this case means a 1-year accumulation period so the value of October 1st represents the average SPI of the 12 months before this date. The raw data was assembled in 1°x1° grids in map form and clipped to the reservoirs. The mean in the reservoir was taken as the predictor value.

Reservoir levels: Reservoir levels were obtained from SNIRH as the end-of-day values (23:00 h) where I extracted only the last value of a month to get an average of the hydrological year. Not more values were used (e.g., daily), as end-of-month values were usually the only ones supervised and other values contained faulty measurements. Pre-fire, Fire, post-fire, and 2-year-post-fire hydrological years were considered in the same way as with the SPI12. The measurements taken ranged however from October 31st to September 30th in the following year.

A.4 Missing data before multiple imputation in the predictor and response variables

The proportion of missingness indicates the percentage of the proportion of missing cases/total cases, the fraction of missing information determines how much of the variance of a variable where data is missing could be regressed through other variables, with higher numbers suggesting a higher amount of lost information through missing data points in the variable (Table AT.1). The fraction of missing information for the fire severity variables on average is lower than in the reservoir levels, since fire severity was correlated with, and can therefore be regressed from fire size.

Table AT.1: Information on missing data of the predictors. SPI12 represents the standardized precipitation index with a 12-month accumulation period. The index of connectivity (IC) is represented through the 75th percentile, and fire severity through the burned area above a certain Δ normalized burn ratio (NBR).

Predictor	Proportion of missingness (%)	Fraction of missing information
Fire size	0	0
Watershed-area-to-volume-ratio	0.84	0.003
Aridity Index (2000-2010)	0	0
pre-fire Reservoir level	28.57	0.535
fire-year reservoir level	27.73	0.255
post-fire reservoir level	26.05	0.341
2-year post-fire reservoir level	26.89	0.213

pre-fire SPI12	0.84	0
fire-year SPI12	0.84	0
post-fire SPI12	0	0
Land-use predictors (all combined)	0	0
Fire severity (area $\geq 0.27 \Delta\text{NBR}$)	31.09	0.032
Fire severity (area $\geq 0.44 \Delta\text{NBR}$)	31.09	0.272
Fire severity (area $\geq 0.66 \Delta\text{NBR}$)	31.09	0.2
IC 75th quantile	19.33	0.268

Fraction of missing information in the response was not calculated because it is related to correlation, which was not established as having a predictive effect (Table AT.2). Only COD had a possibly significant proportion of missingness.

Table AT.2: Proportion of missingness in the response parameters of biological oxygen demand (BOD), chemical oxygen demand (COD), conductivity (COND), total phosphorus (TP), nitrate (NO₃), dissolved oxygen (DO), total suspended sediments (TSS), and pH. All parameters show low levels of missingness except for COD.

Response	Proportion of missingness (%)
BOD	3.36
COD	10.08
COND	0
TP	3.36
NO ₃	0
DO	1.68
TSS	0.84
pH	0.84

A.5 PCA and Cluster analysis of predictors:

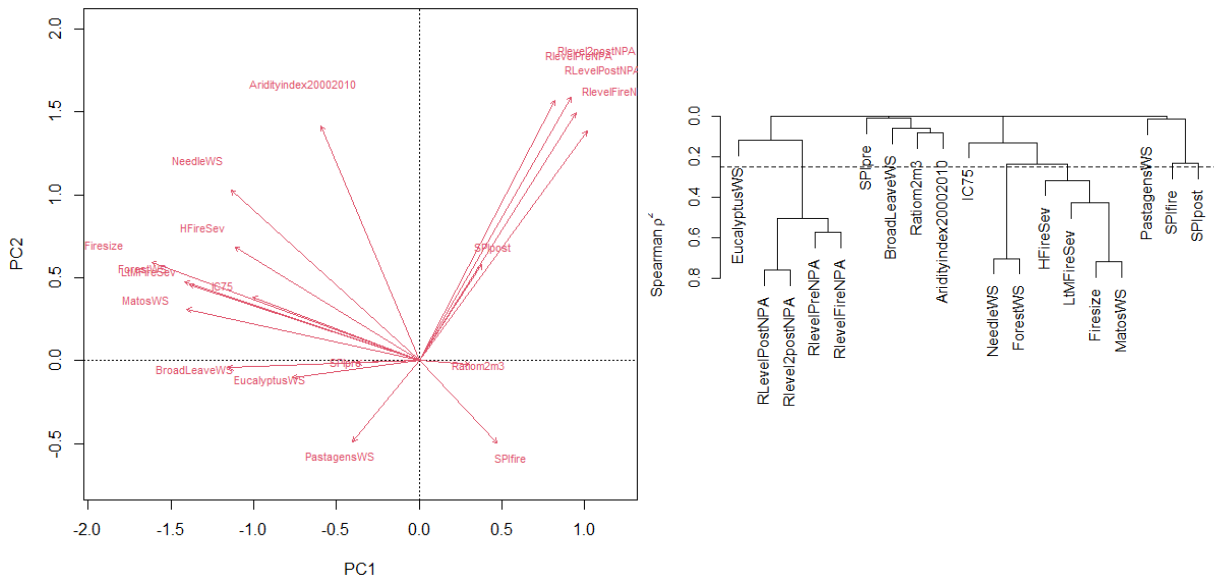


Figure AF.2: PCA (left) and Cluster analysis (right) of the predictors. The dashed line in the cluster analysis shows the $r > 0.5$ cut-off. Note that correlation values are shown in r^2 , so the cut-off lies at 0.25 in the graphic.

Reservoir levels from different years are highly correlated both in the PCA and the cluster analysis (Figure AF.2: PCA (left) and Cluster analysis (right) of the predictors). The dashed line in the cluster analysis shows the $r > 0.5$ cut-off. Note that correlation values are shown in r^2 , so the cut-off lies at 0.25 in the graphic. Figure AF.2) while another major cluster can be found around fire size, fire severity, IC, and some land use variables. Both, the PCA and cluster analysis suggest similar clusters. Even though the Forest/Needle cluster is just under a correlation of 0.5 in the cluster analysis, these predictors were added to the fire size/severity cluster and therefore not used simultaneously in the models. The same was done with the SPI12 fire year/SPI12 post-fire year cluster.

A.6 Results of the changepoint analysis

Table AT.3: Results of the changepoint analysis for the parameters biological oxygen demand (BOD), chemical oxygen demand (COD), conductivity (COND), total phosphorus (TP), nitrate (NO3), dissolved oxygen (DO), total suspended sediments (TSS), and pH. Orange marks a changepoint with an increase in value/concentration, while blue marks a decrease. The white spots are NAs and grey marks no changepoint in the event.

Reservoir	Fire date	Fire size %	BOD	COD	Cond.	P	NO3	DO	TSS	pH
AGUIEIRA	1998	8.199								
AGUIEIRA	2005	6.955								
AGUIEIRA	2010	5.251								
AGUIEIRA	2017	43.868								
ALTO RABAGAO	1998	6.472								
ALTO RABAGAO	2005	9.774								
ALTO RABAGAO	2011	4.295								
ALTO RABAGAO	2017	3.767								
ALVAO	2009	32.134								
ALVITO	2001	0.202								
ALVITO	2012	0.269								
APARTADURA	2003	53.347								
ARADE	2003	53.844								
ARADE	2018	54.088								
AZIBO	2015	4.247								
BASTELO	2000	0.473								
BASTELO	2009	1.117								
BELICHE	2004	41.584								
BELICHE	2012	2.828								
BRAVURA	1995	0.782								
BRAVURA	2003	81.257								
BRAVURA	2015	1.77								
CABRIL	2017	24.448								
CAIA	1985	9.455								
CAIA	2003	1.003								
CALDEIRAO	2016	2.51								
CAMBA	1999	3.862								
CAMBA	2011	2.476								
CAMBA	2017	5.198								
CANICADA	1998	6.874								
CANICADA	2010	19.122								
CANICADA	2017	7.202								
CAPINHA	2016	0.237								
CASTELO BODE	2003	45.696								
CASTELO BODE	2017	32.944								
CORGAS	2011	10.882								
COVA DO VIRIATO	2017	30.122								
DIVOR	2003	2.204								
DIVOR	2016	0.242								
ENXOE	2001	0.167								
FAGILDE	2005	8.53								
FAGILDE	2013	10.304								
FONTE LONGA	2000	0.219								
FRONHAS	2005	19.665								
FRONHAS	2012	6.642								
FRONHAS	2017	51.636								
FUNCHO	2004	33.341								
FUNCHO	2018	6.07								
LAPA	2017	37.21								
LUCEFECIT	2006	10.811								
MAGOS	2004	0.215								
MAGOS	2016	0.194								
MARANHAO	2003	1.505								
MARANHAO	2013	0.32								
MARATECA	2005	8.183								
MARATECA	2017	22.576								
MEIMOA	2005	2.554								
MEIMOA	2011	0.438								
MONTE NOVO	2003	0.982								
MONTE NOVO	2015	0.159								
MONTE ROCHA	2003	2.092								

Reservoir	Fire date	Fire size %	BOD	COD	Cond.	P	NO3	DO	TSS	pH
ODELEITE	2004	10.44								
ODELEITE	2012	37.194								
ODIVELAS	2003	0.303								
OLGAS	2017	8.4								
PARADELA	2005	3.75								
PARADELA	2011	14.825								
PARADELA	2017	6.924								
PATUDOS	2003	8.275								
PEGO ALTAR	2003	1.104								
PEGO ALTAR	2010	0.26								
PENEDO REDONDO	2017	87.389							*	
PENEIREIRO	2014	21.113								
PENHA GARCIA	2015	0.6								
PISAO	2017	3.215								
PISCO	2005	44.541								
POVOA MEADAS	1991	2.217								
POVOA MEADAS	2003	43.958								
PRACANA	2017	14.654								
PRETAROUCA	2017	25.844								
RAIVA	2005	4.68								
RANHADOS	2006	11.863								
RANHADOS	2013	3.846								
ROXO	1998	0.291								
ROXO	2005	0.424								
SABUGAL	2009	2.43								
SABUGAL	2017	0.299								
SALAMONDE	1999	12.056								
SALAMONDE	2005	3.438								
SALAMONDE	2011	16.833								
SALAMONDE	2017	9.656								
SANTA CLARA	2003	1.106								
SANTA CLARA	2015	0.575								
SANTA LUZIA	2005	65.047								
SANTA LUZIA	2017	22.827								
SANTA MARIA AGUIAR	2009	0.522								
SANTA MARIA AGUIAR	2017	2.855								
SAO DOMINGOS	2002	3.863								
SAO DOMINGOS	2012	1.137								
SAO DOMINGOS	2017	1.628								
SERRA SERRADA	2012	32.473								
SORDO	1998	4.42								
SORDO	2009	5.682								
TAPADA GRANDE	2000	0.458								
TOULICA	2015	0.483								
VALE DO GAIO	2003	1.383								
VALE FERREIROS	2000	3.94								
VALE FERREIROS	2012	5.728								
VALE FERREIROS	2017	11.221								
VASCOVEIRO	2011	2.662								
VASCOVEIRO	2017	19.895								
VENDA NOVA	1998	2.722								
VENDA NOVA	2011	5.511								
VENDA NOVA	2017	5.057								
VIGIA	2002	2.439								
VILA CHA	2000	29.309								
VILA CHA	2017	69.437								
VILARINHO DAS FURNAS	2000	3.908								
VILAR TABUACO	2017	9.488								

* The TSS CP of Penedo Redondo was identified by establishing a correlation between TSS and turbidity. No measurements for TSS were available in 2017, but there were simultaneous measurements of TSS and turbidity slightly before and after the 2017 event, while turbidity was measured throughout 2017. A significant spearman correlation of $\rho = 0.835$ with a p-value < 0.001 was found. The validity of using turbidity to determine TSS is discussed e.g., in Rügner et al. (2013). This reservoir was the only reservoir where a proxy was used, as it was important to include because of its large BAR and because TSS was usually more available than turbidity in other reservoirs.